Microstructural characterization of tested AISI 316L tensile specimens from the second operational target module at the Spallation Neutron Source

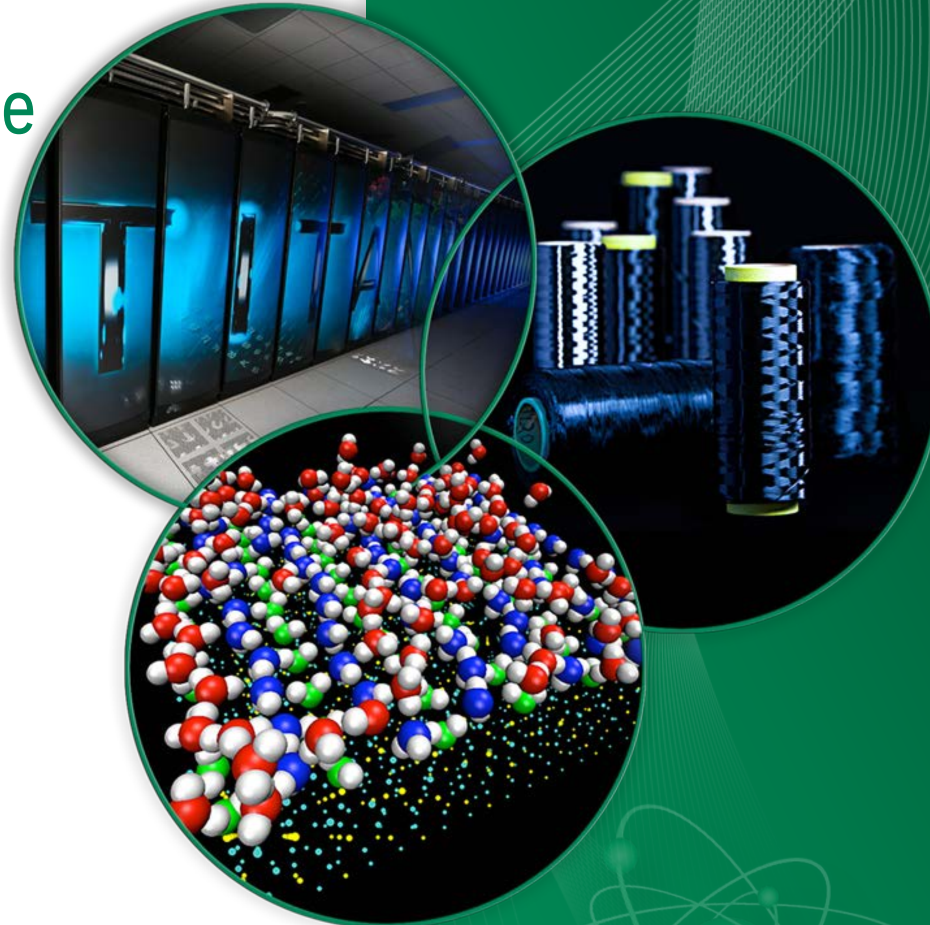

David A. McClintock

Maxim N. Gussev

Oak Ridge National Laboratory

12th International Workshop on Spallation Materials Technology

The Spallation Neutron Source is a megawatt class accelerator-based pulsed neutron source

- Neutrons are produced via high-energy spallation reactions induced by injecting 1 GeV protons into liquid mercury at a frequency of 60 Hz

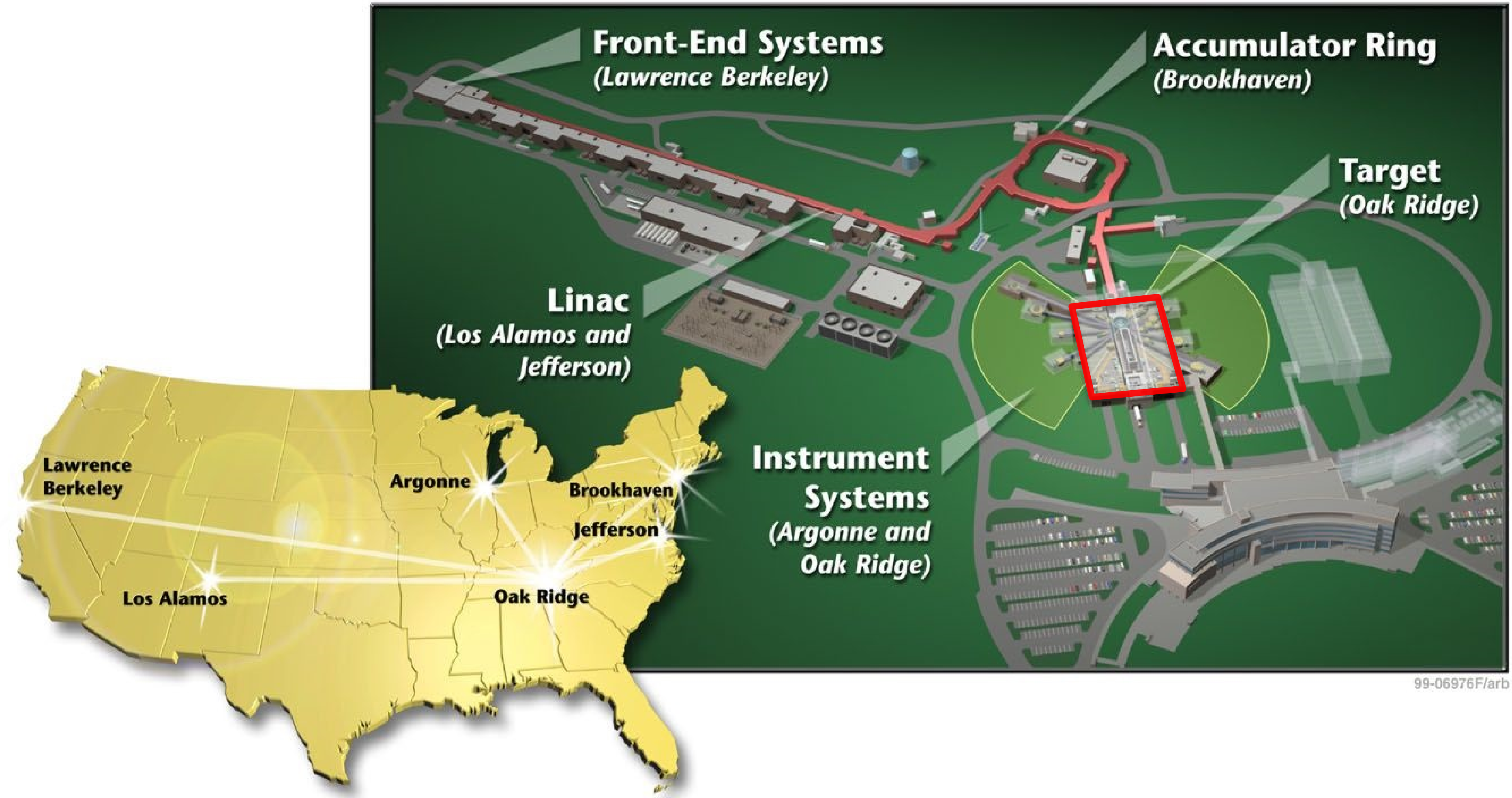

The target provides neutrons to 24 beam lines

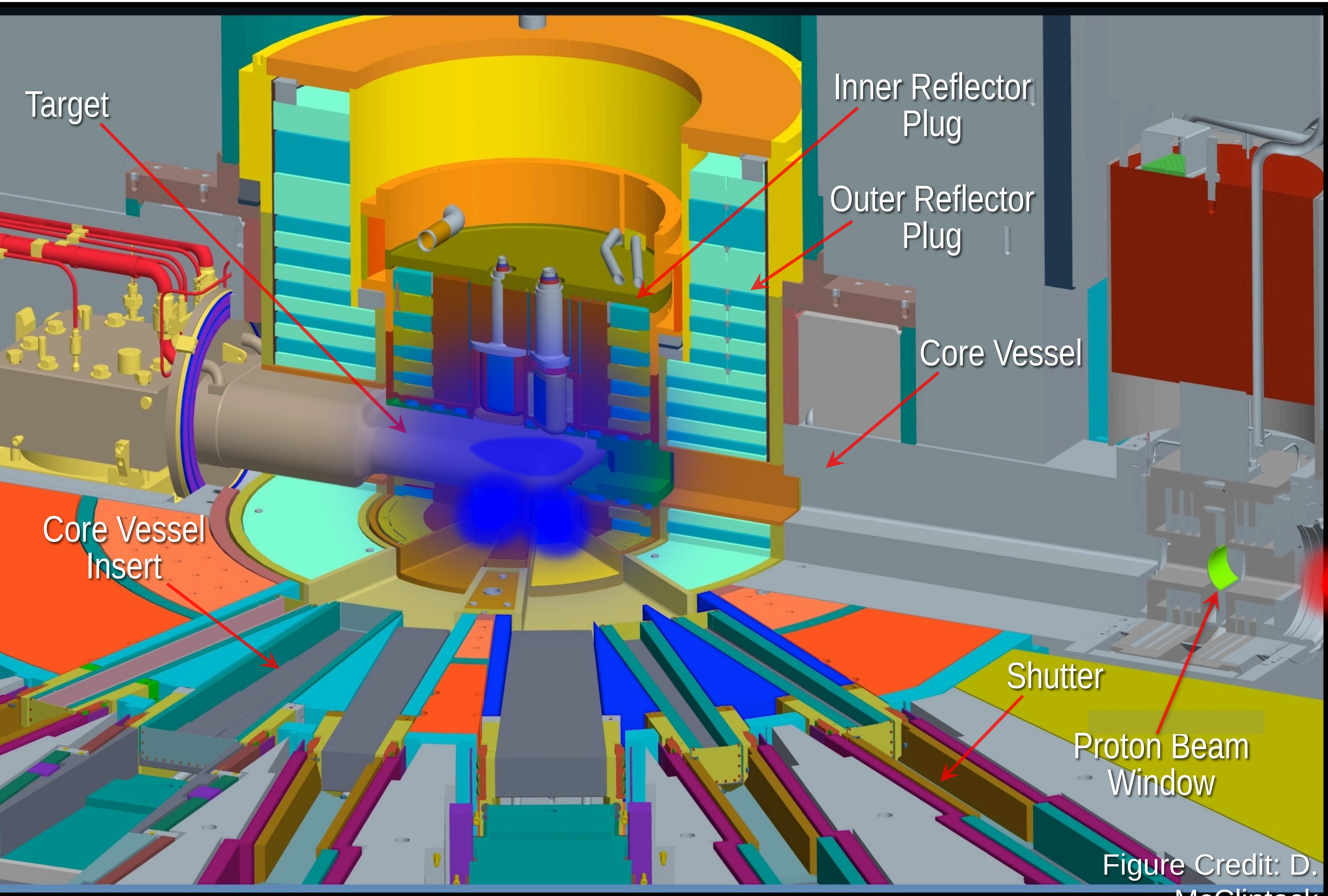

Disk-shaped specimens were removed from beam entrance region of targets after service

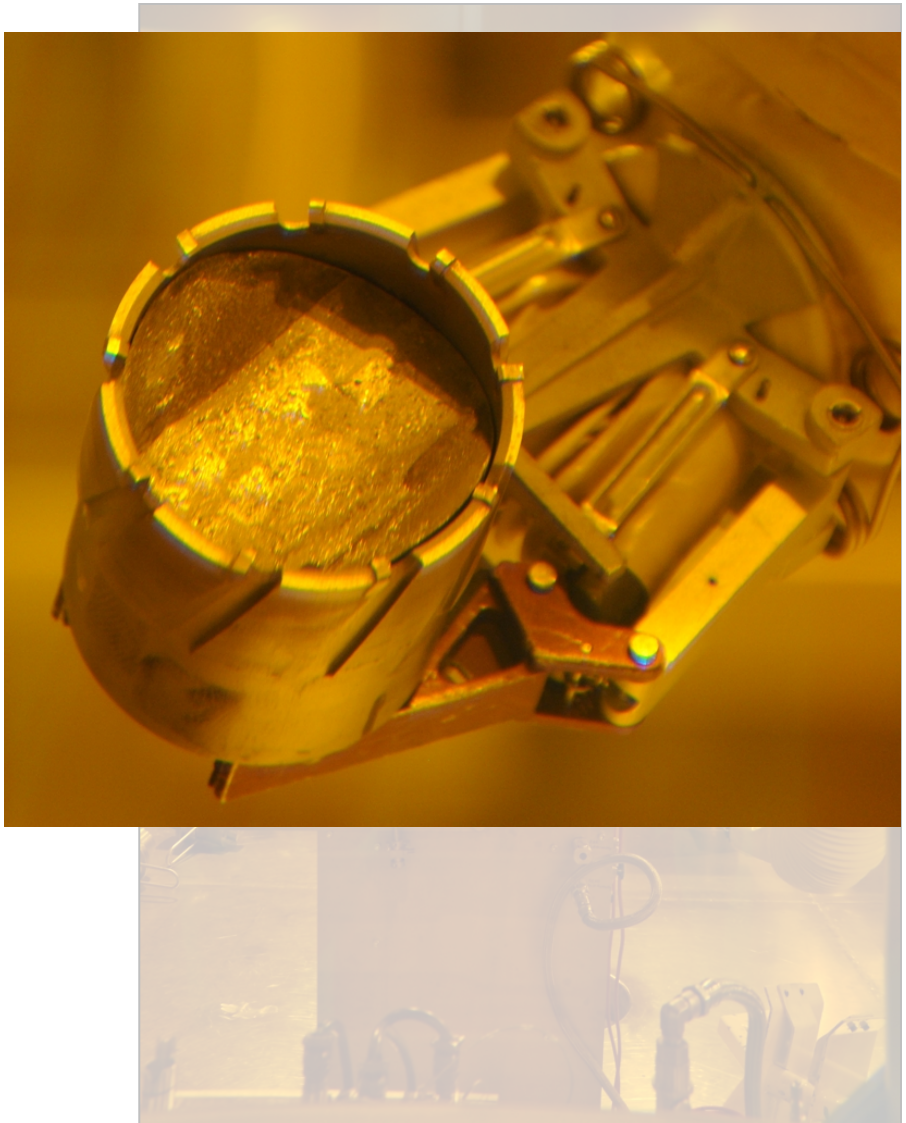

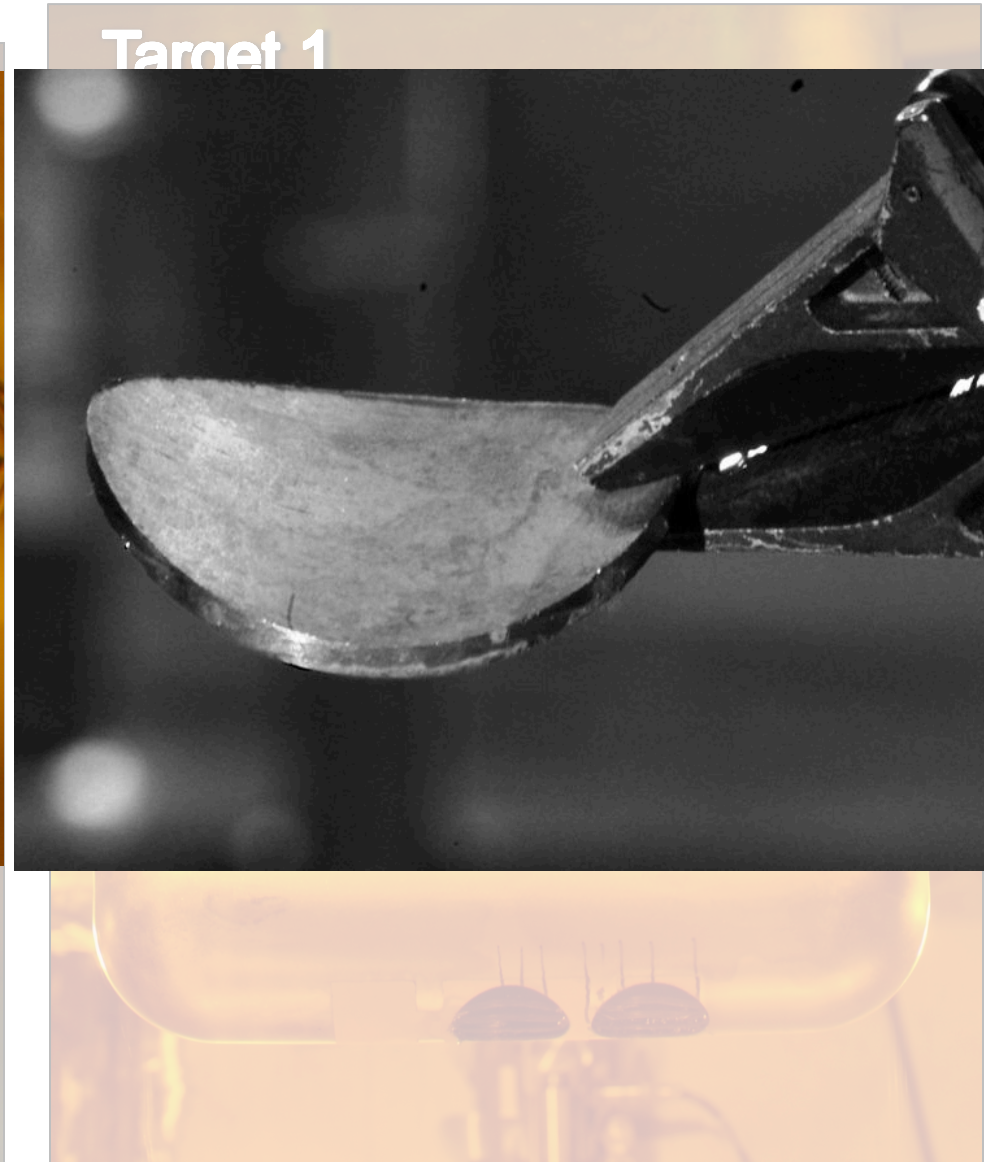

Figure Credit: D. McClintock

Target Sampling

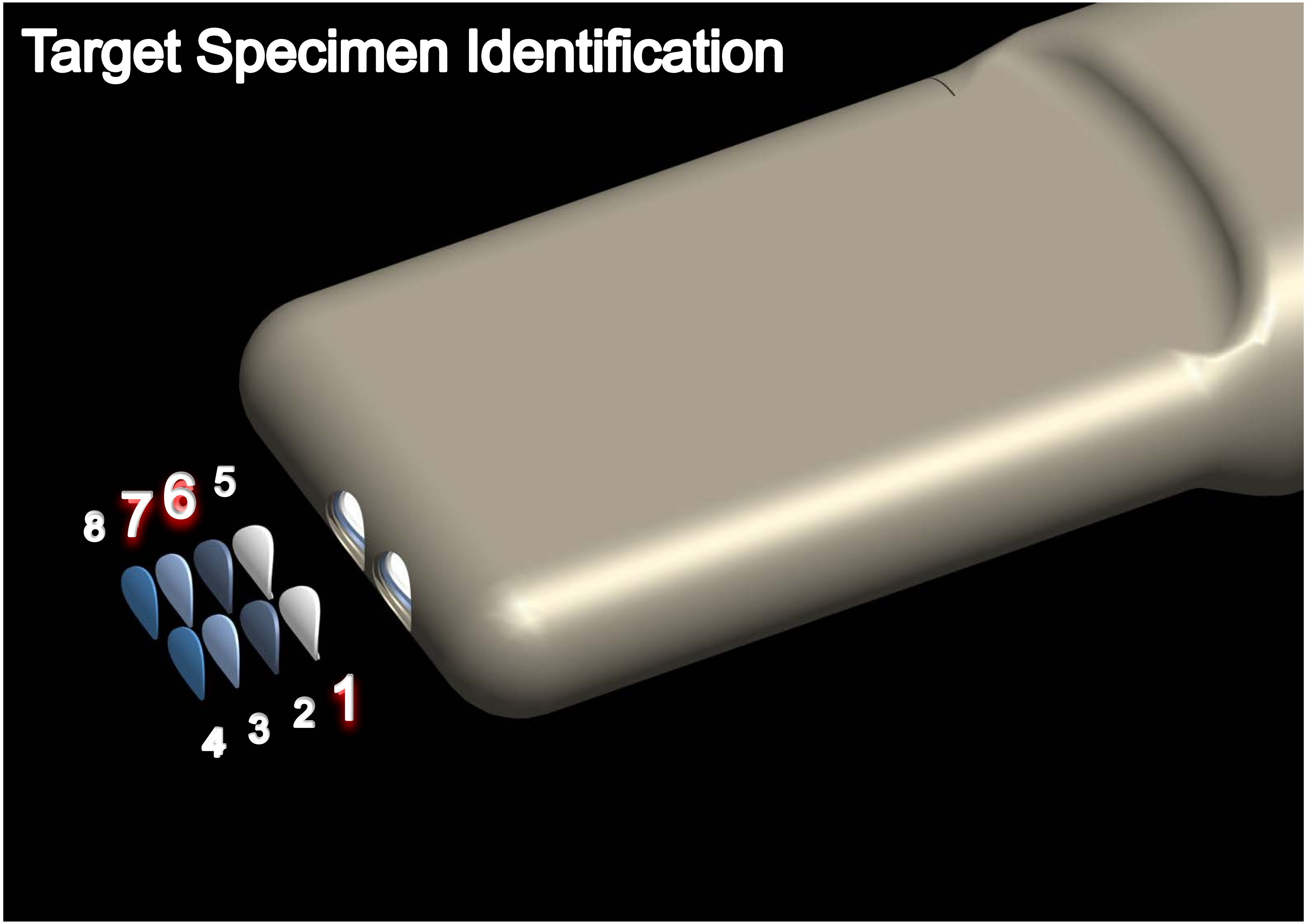

Tensile Specimen Fabrication

- The tensile specimens were fabricated and tested by Babcock & Wilcox Technical Services Group (Lynchburg, VA, USA)
- The disks were cleaned in an ultrasonic bath and photographed; the images were used to produce specimen maps for each disk
- Specimen machining maps were produced for each disk and the specimens were machined via electrical-discharge machining (EDM)

<u>Example: Disk 6 from Target 2</u>

Before Cleaning

After Cleaning

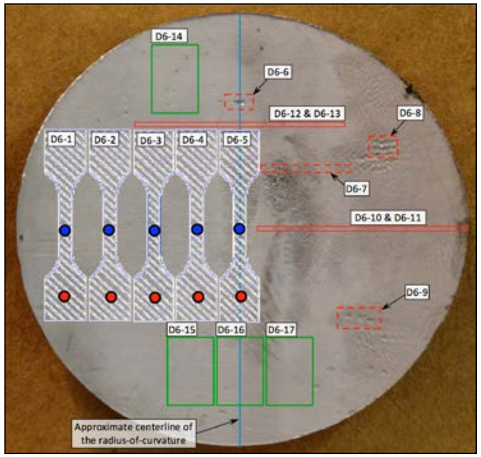

Specimen Map

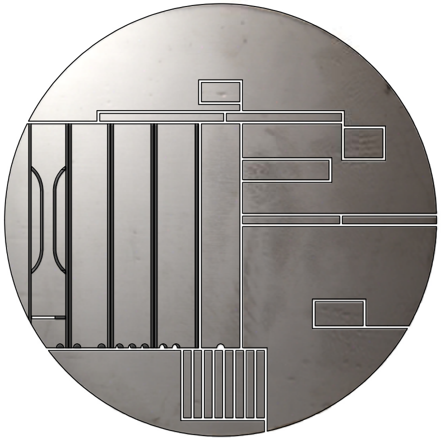

EDM Machining Map

Tensile data show significant strengthening occurred during operation

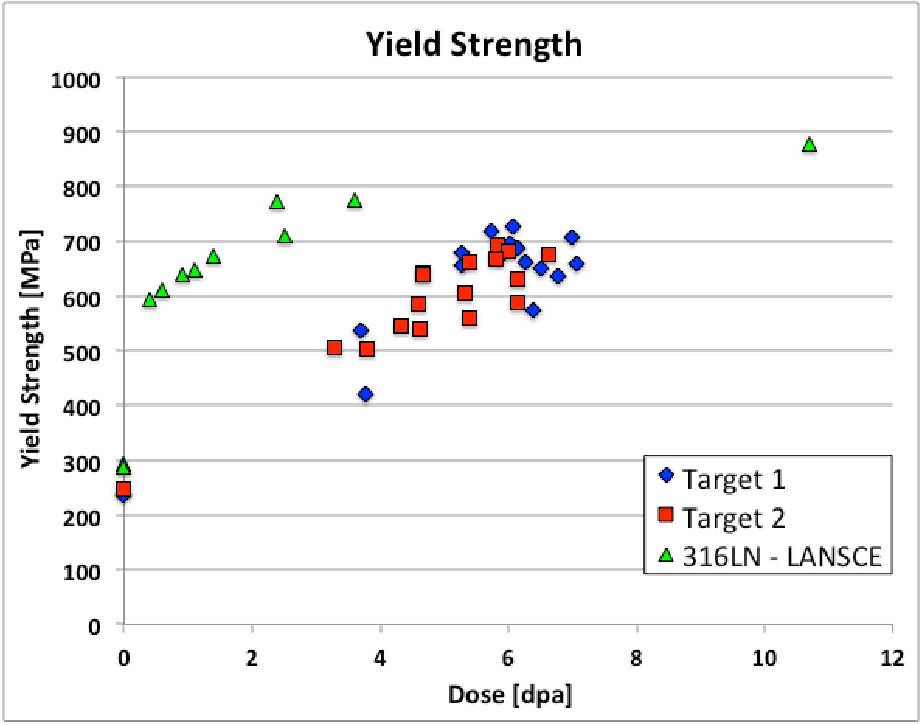

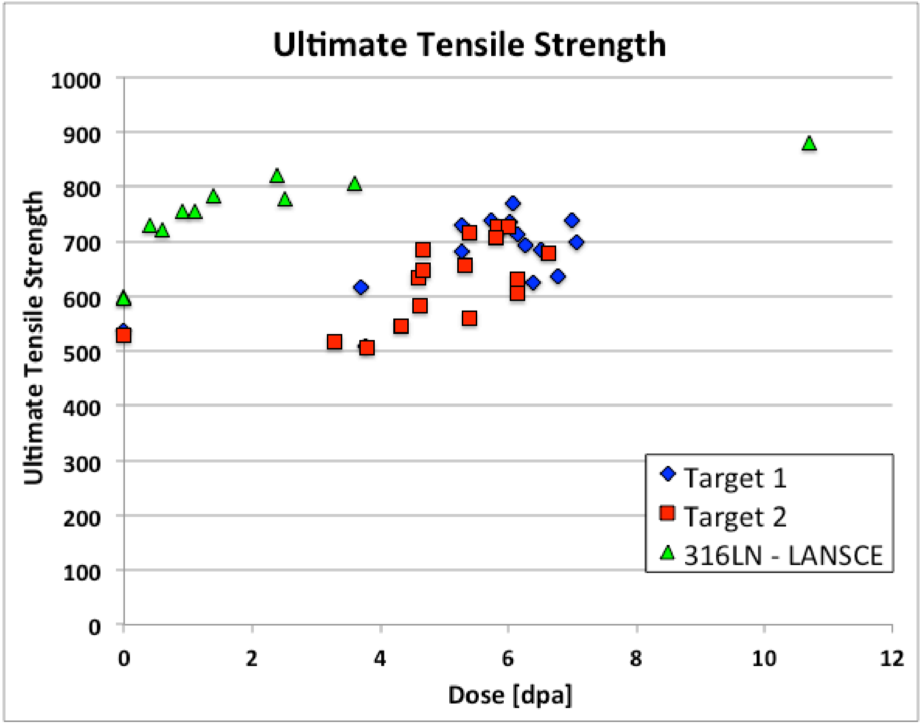

- LANSCE irradiation* was 316LN – slight higher strength expected due to nitrogen addition
- General hardening trend of SNS tensile data is consistent with data in literature

Figures Reproduced From: D.A. McCintock et al., *Journal of Nuclear Materials* 450 (2014) 130-140

*K. Farrell and T.S. Byun, *Journal of Nuclear Materials*, 296 (2001) 129-138

Tensile data show appreciable total elongation ... ren...

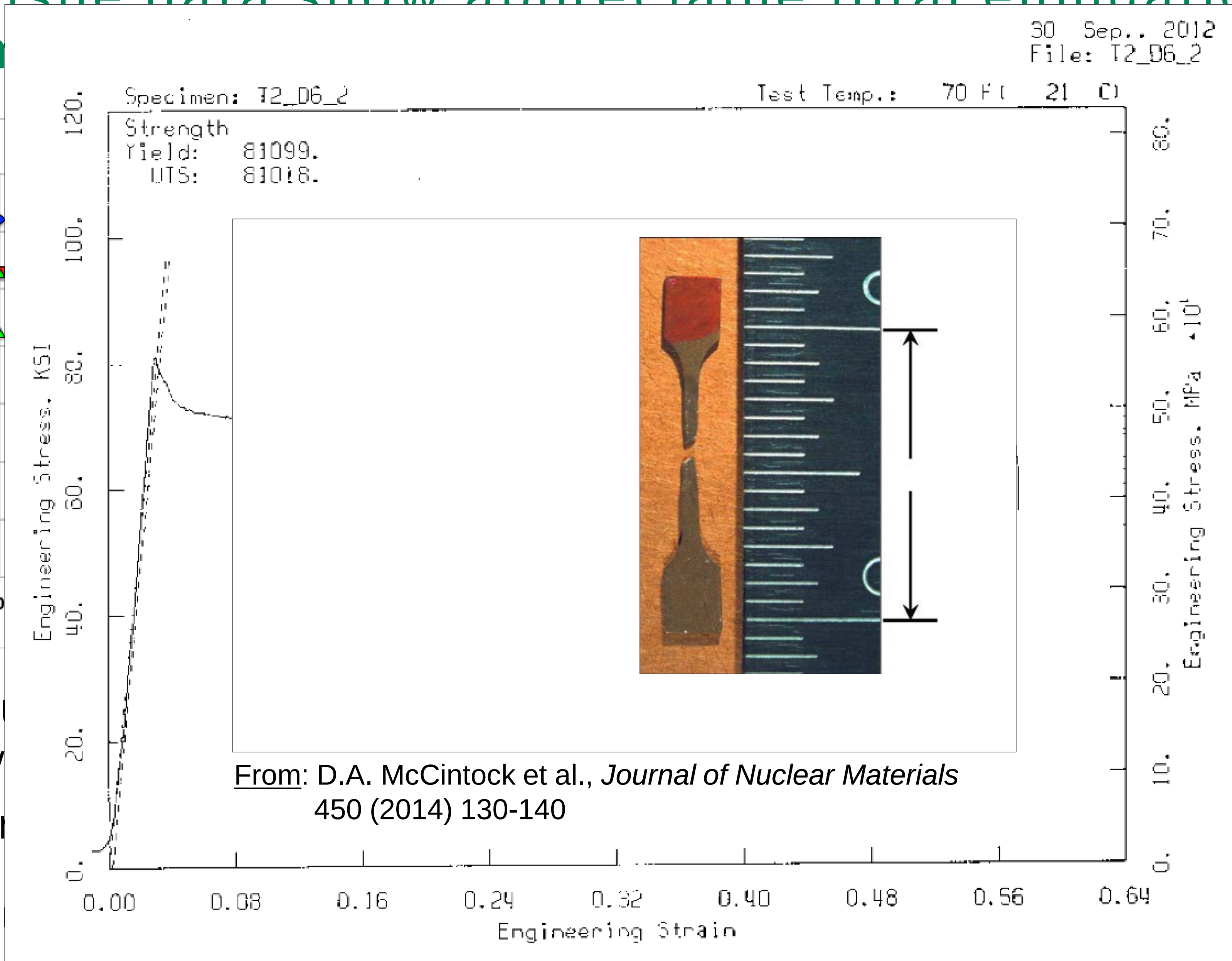

From: D.A. McCintock et al., *Journal of Nuclear Materials* 450 (2014) 130-140

Uniform Elongation [%]

70 60 50 40 30 20 10 0

0 ... 12

LANSCE

- Redu... ...nt with prev...
- Appr... ...gation

Figures ...

Inability to neck produces a "deformation wave" in highly irradiated stainless steel*

*Slide Courtesy of: Frank Garner and Maxim Gusev

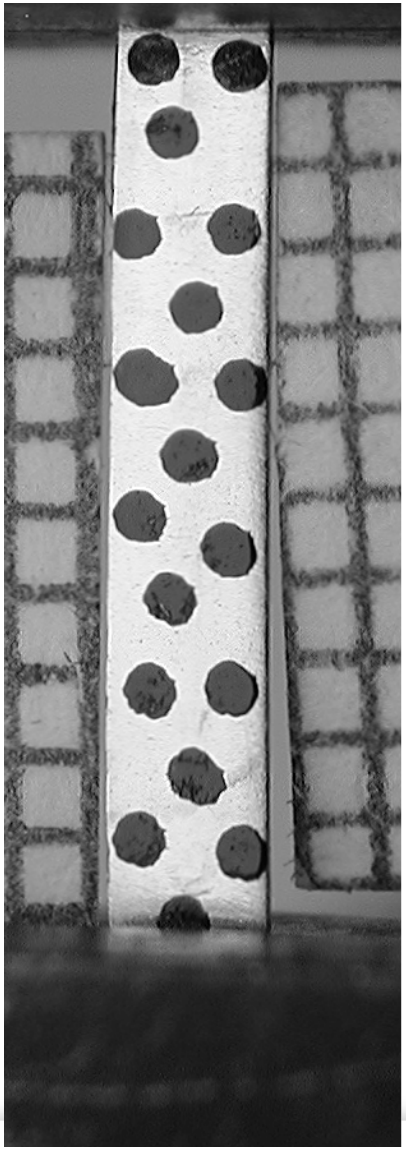

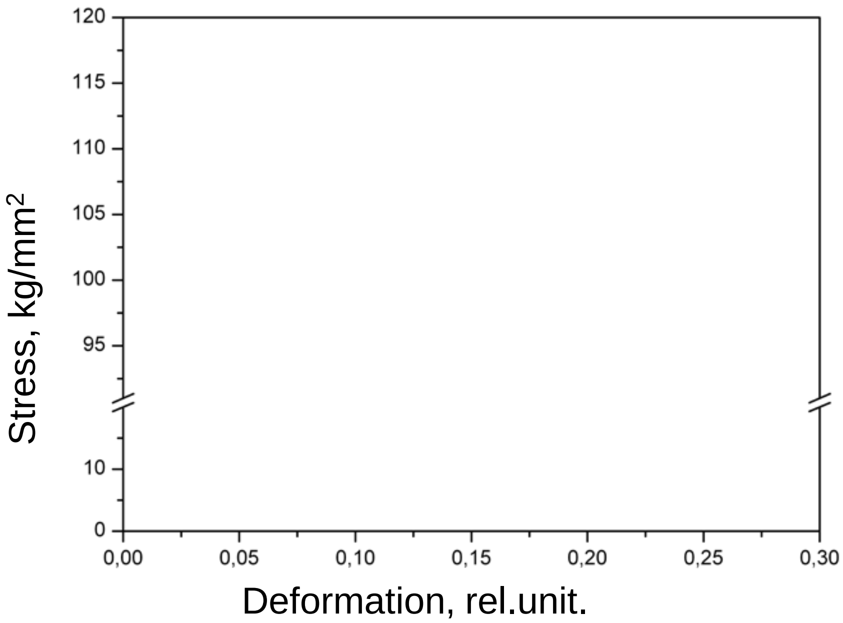

55 dpa, 310° C
in BN-350

Russian analog to 321 stainless steel

room temperature test

A "deformation wave" appears on the surface and moves along the specimen gauge section

Gusev et al., J. Nucl. Mater. 386–388 (2009) 273–276
Gusev et al., J. Nucl. Mater. 403 (2010) 121–125

Three specimens from Target 2 were selected for microstructural characterization

D1-2

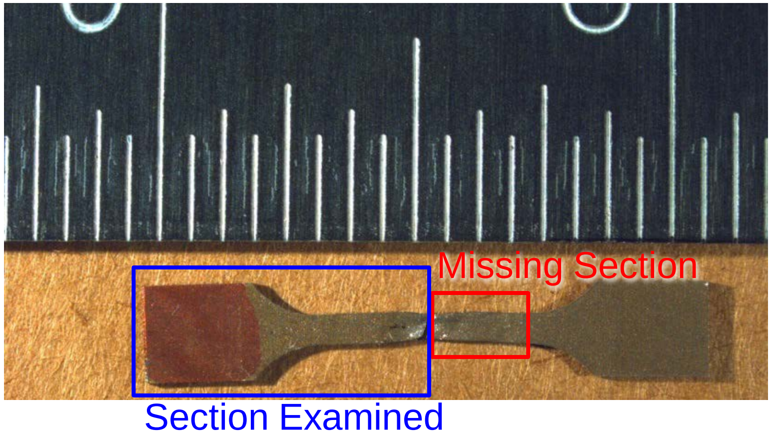

D7-2

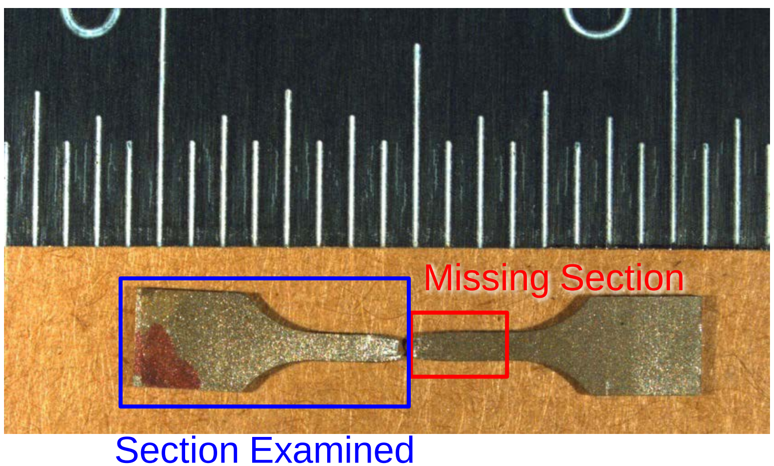

D6-2

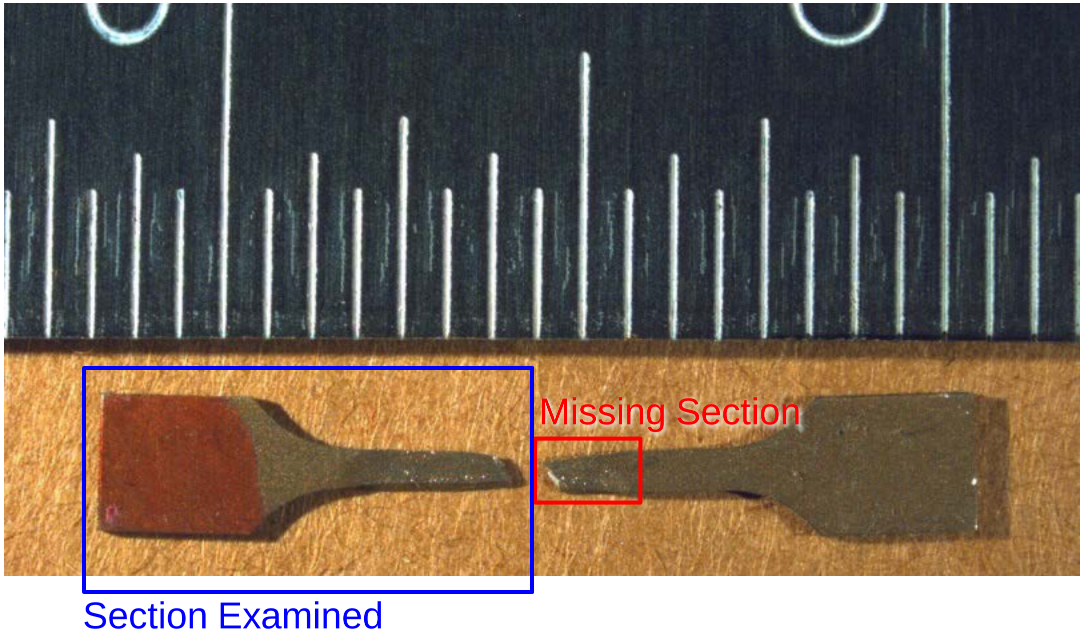

The D6-2 specimen was of utmost interest:

- Strong non-uniform deformation along the gauge.
- An evidence of a Luders band or deformation wave phenomena?

The three Target 2 specimens chosen for examination displayed different tensile behavior

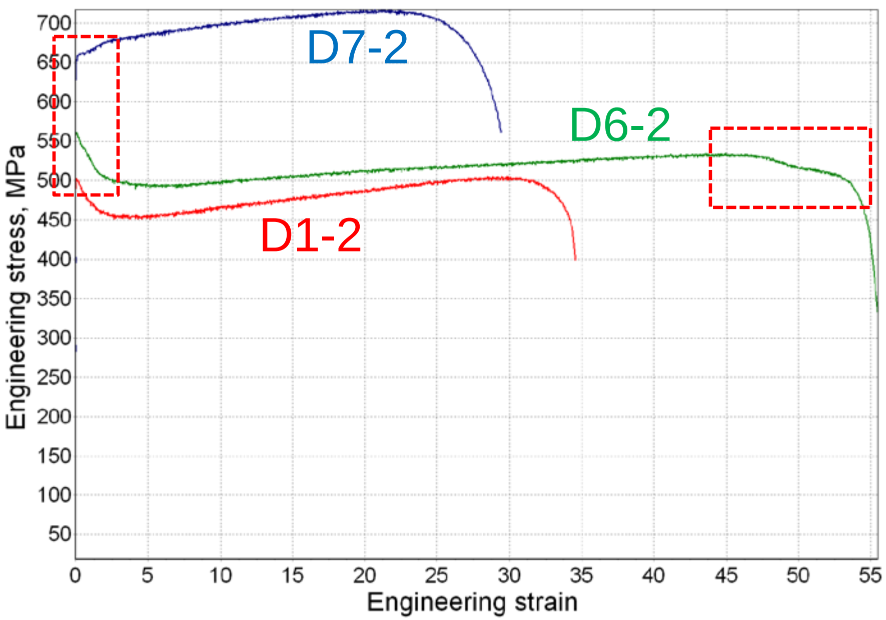

Three tensile specimens with similar damage dose level were selected for microstructure characterization.

- D7-2 vs. D1-2: similar ductility but different strength level.
- D1-2 vs. D6-2: similar strength level but different ductility values and plastic behavior during necking.
- D7-2 vs. (D1-2, D6-2): different behavior at the small strain area.

Specimen	Dose [dpa]	Yield Strength [MPa]	Ultimate Strength [MPa]	Fracture Strength [MPa]	Fracture Stress [MPa]	Uniform Elongation [%]	Total Elongation [%]	Reduction in Area [%]
D1-2	3.8	503	505	399	841	32.1	36.7	52.7
D6-2	5.4	558	558	386	653	0	57.1	40.9
D7-2	5.4	661	716	575	1173	24.1	31.9	51

Magnetic Phase (M_f) Measurements

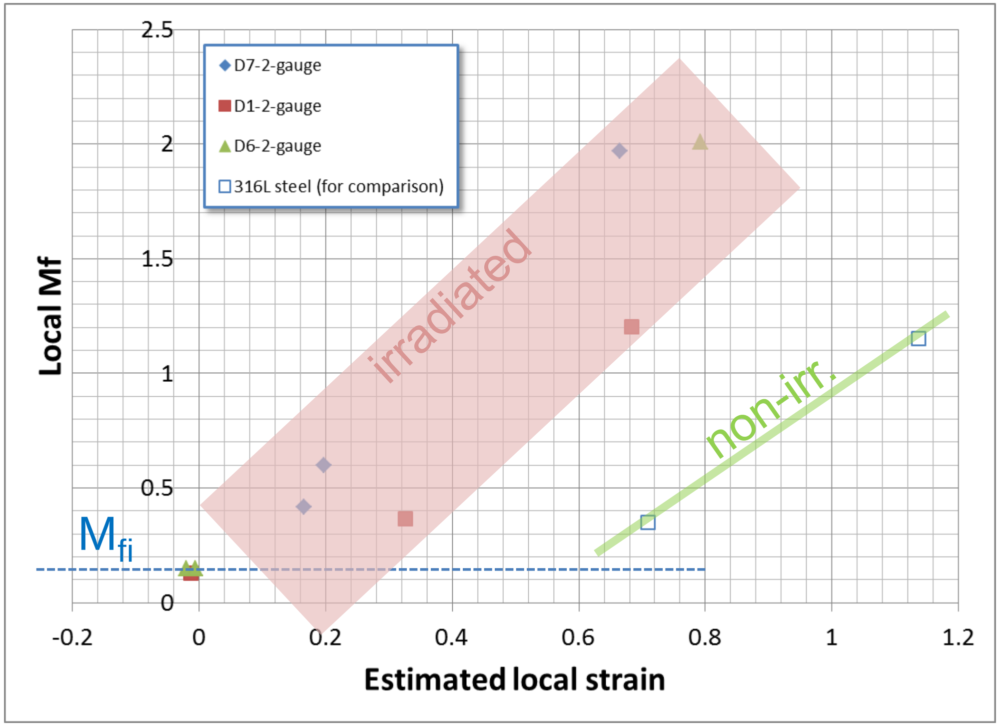

Magnetic phase measurements were conducted using Fisher Ferroprobe unit calibrated with standard etalon samples.

- All irradiated specimens contained some magnetic phase after irradiation (M_{fi}~0.15%; most probably, radiation-assisted ferrite or martensite).
- All specimens demonstrated magnetic phase increase during straining.
- For the same local strain level, the magnetic phase amount in the irradiated specimens was much larger than in the non-irradiated (commercial 316L steel was used for comparison).
- Can we say the irradiated material becomes more unstable?

Strain-induced relief was observed on the surface of specimens

- D6-2 and D1-2 specimens demonstrated pronounced strain-induced relief on specimen surfaces
- Surface relief observations indicate the gauge sections was composed of large “abnormal” grains

Tensile Specimen Gauges Sections with Grains Marked

D6-2

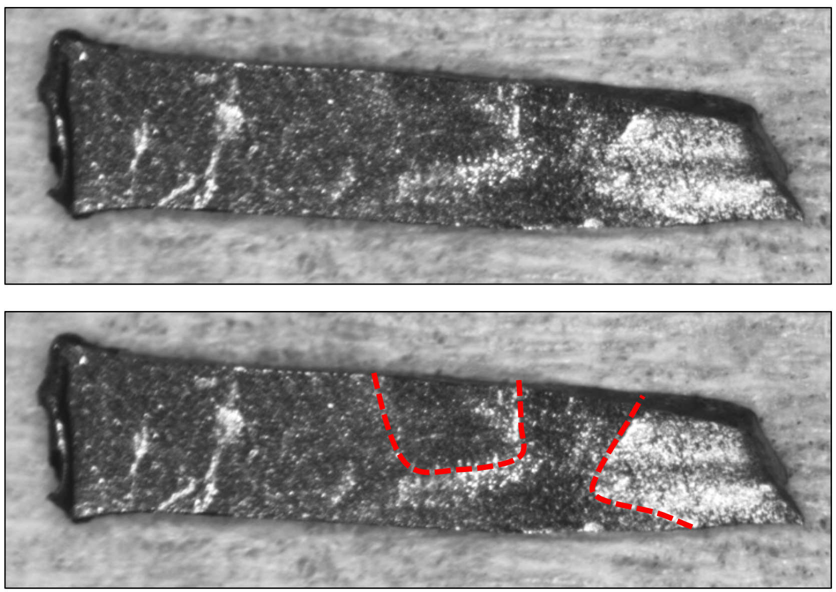

D1-2

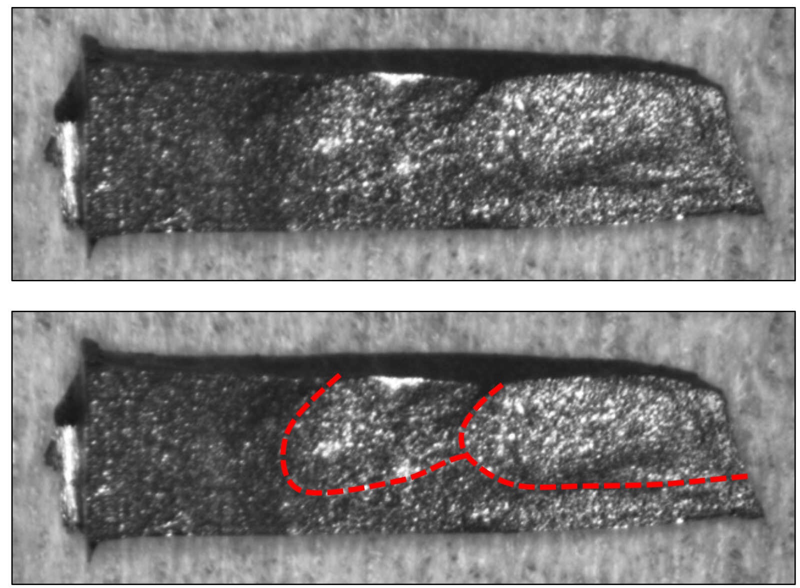

Very large grains were observed in the non-deformed material (D6-2 specimen head)

Pronounced bi-modal grain size distribution, some grains may reach 1.5-2 mm!

EBSD IPF-maps

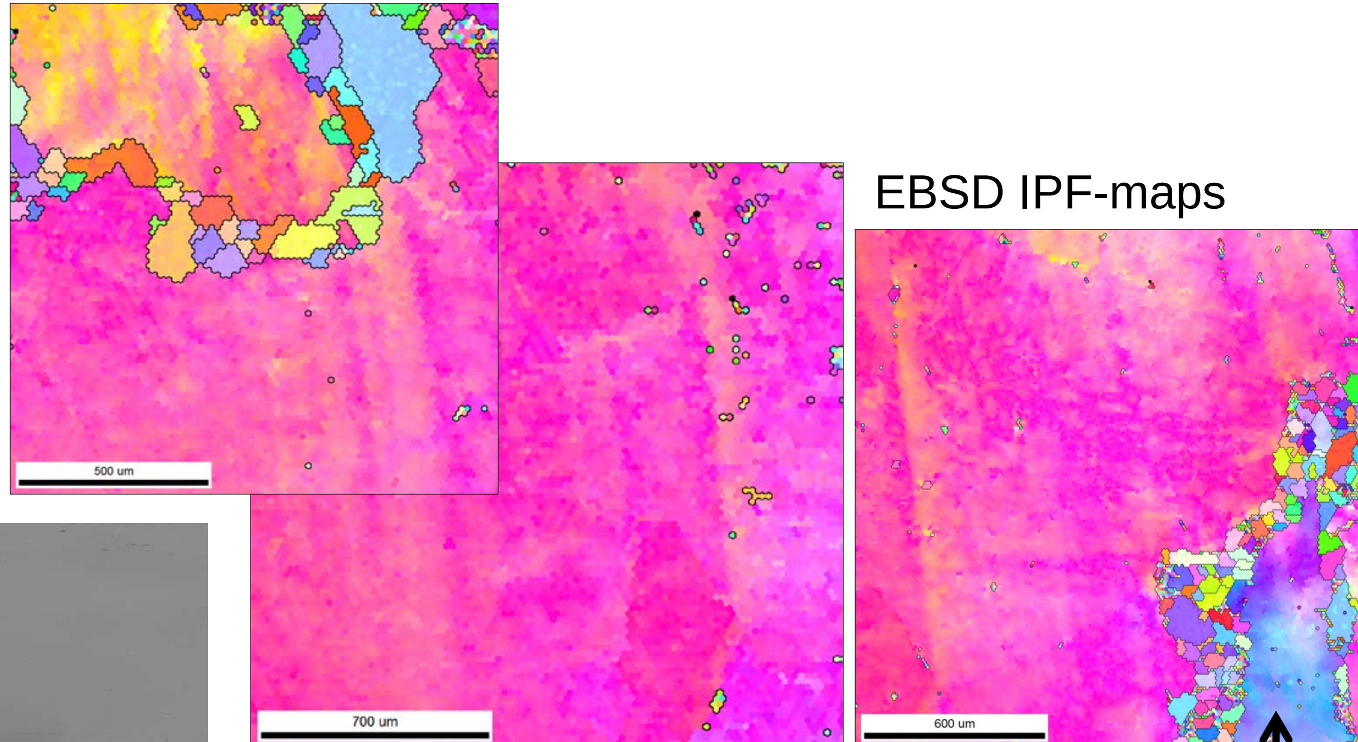

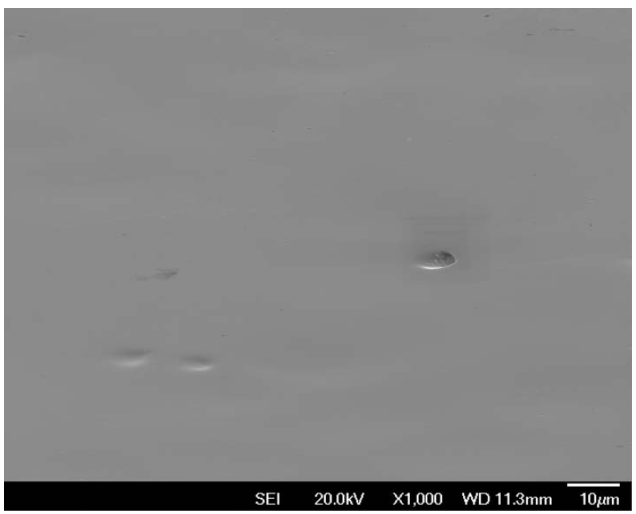

Typical view of the electropolished surface at 1000x

Large grains usually are surrounded by “small grain belt”. EBSD patterns quality is much lower compared to usual annealed and irradiated steel.

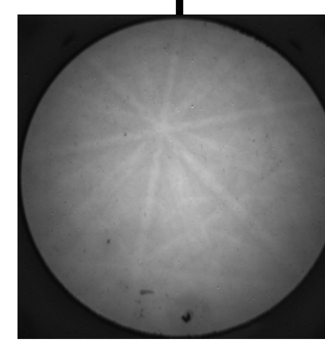

Large in-grain misorientation was observed in large grains

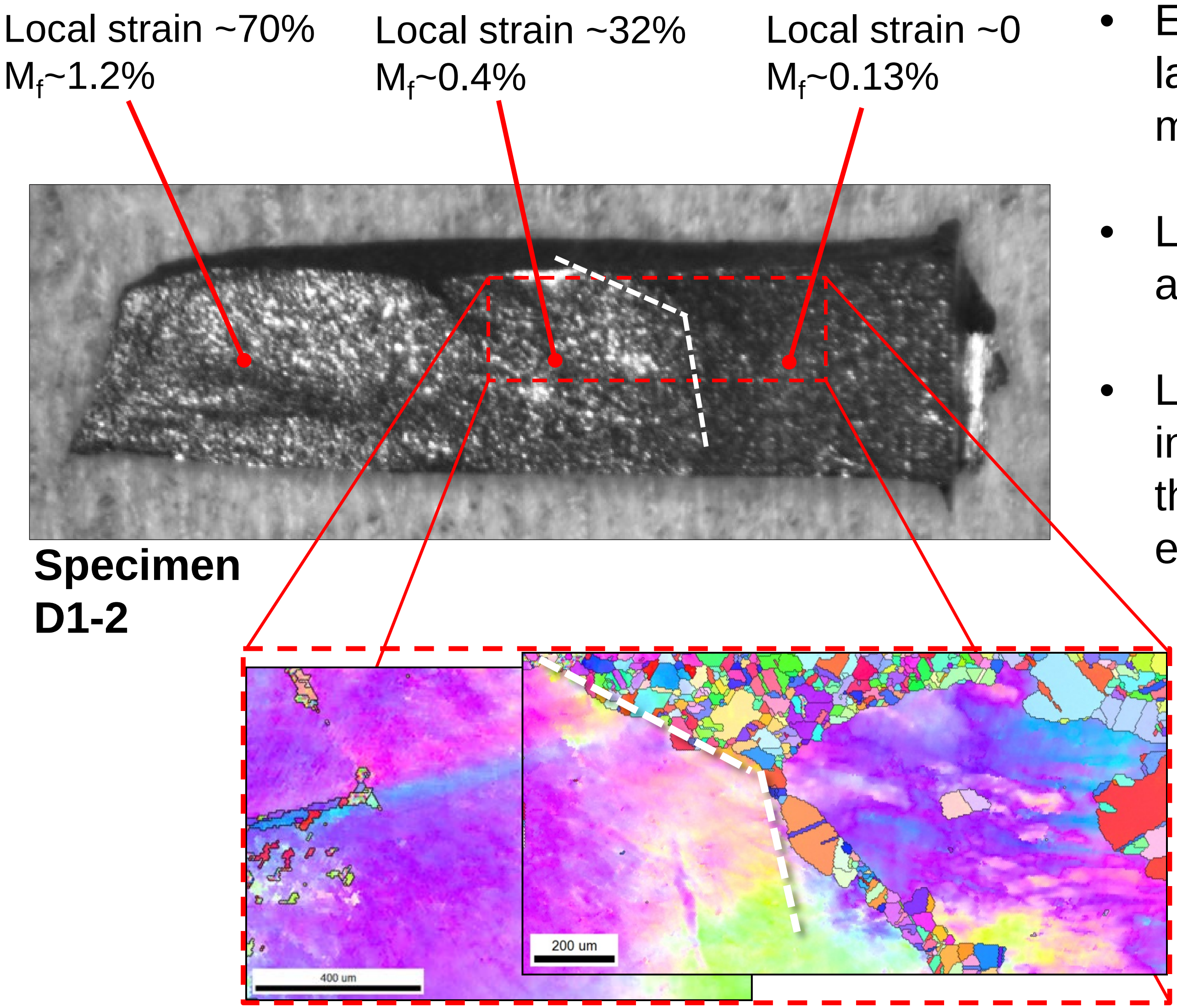

Specimen D1-2

- EBSD demonstrated that large grains are present in material.
- Large grains are embedded in a “shell” of regular grains.
- Large grains have significant in-grain misorientation even if this gauge portion did not experience plastic strain.

Analysis of abnormal grains show internal misorientation

Scan #3, 50x

IPF

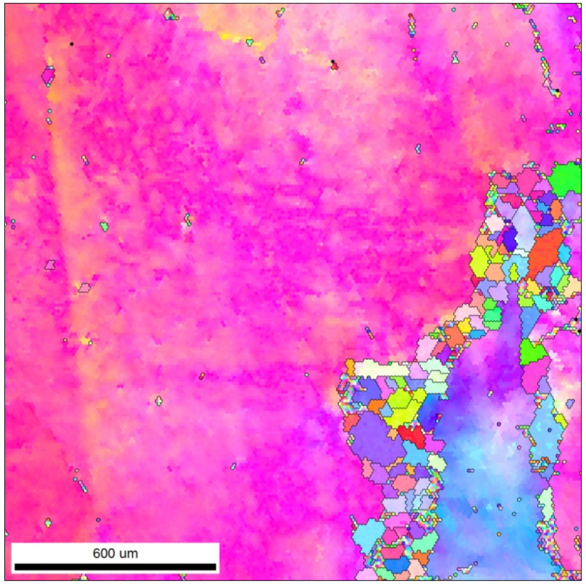

GROD

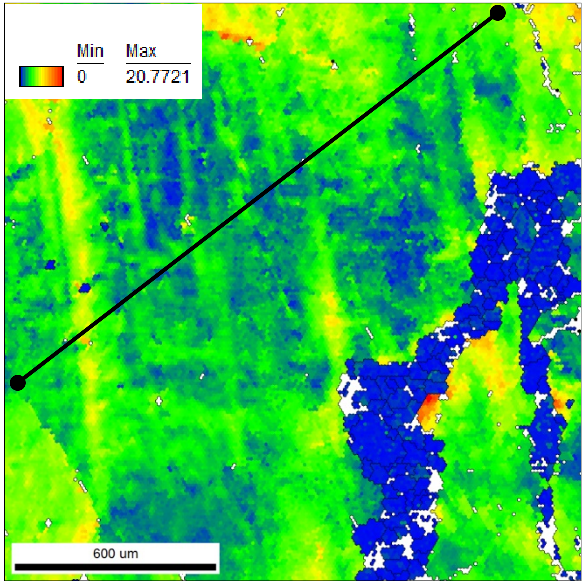

Misorientation profile

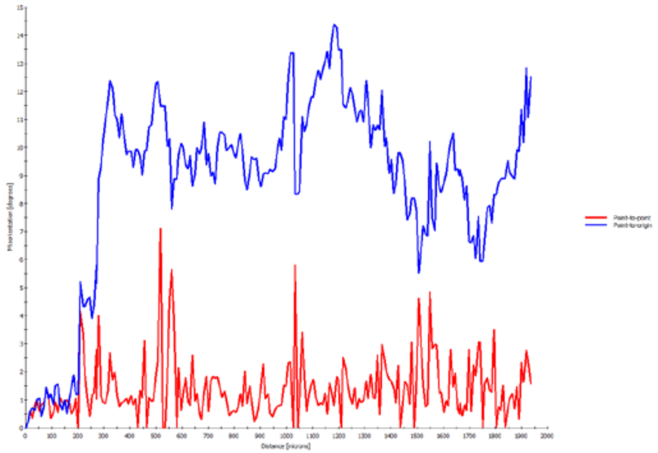

- In all cases, large grains also had significant internal misorientation level
- Often large grains had also multiple internal low-angle boundaries (below 2-3 degree)
- Misorientation should not present in the annealed material

Section of D1-2 near fracture contained significant deformation and misorientation

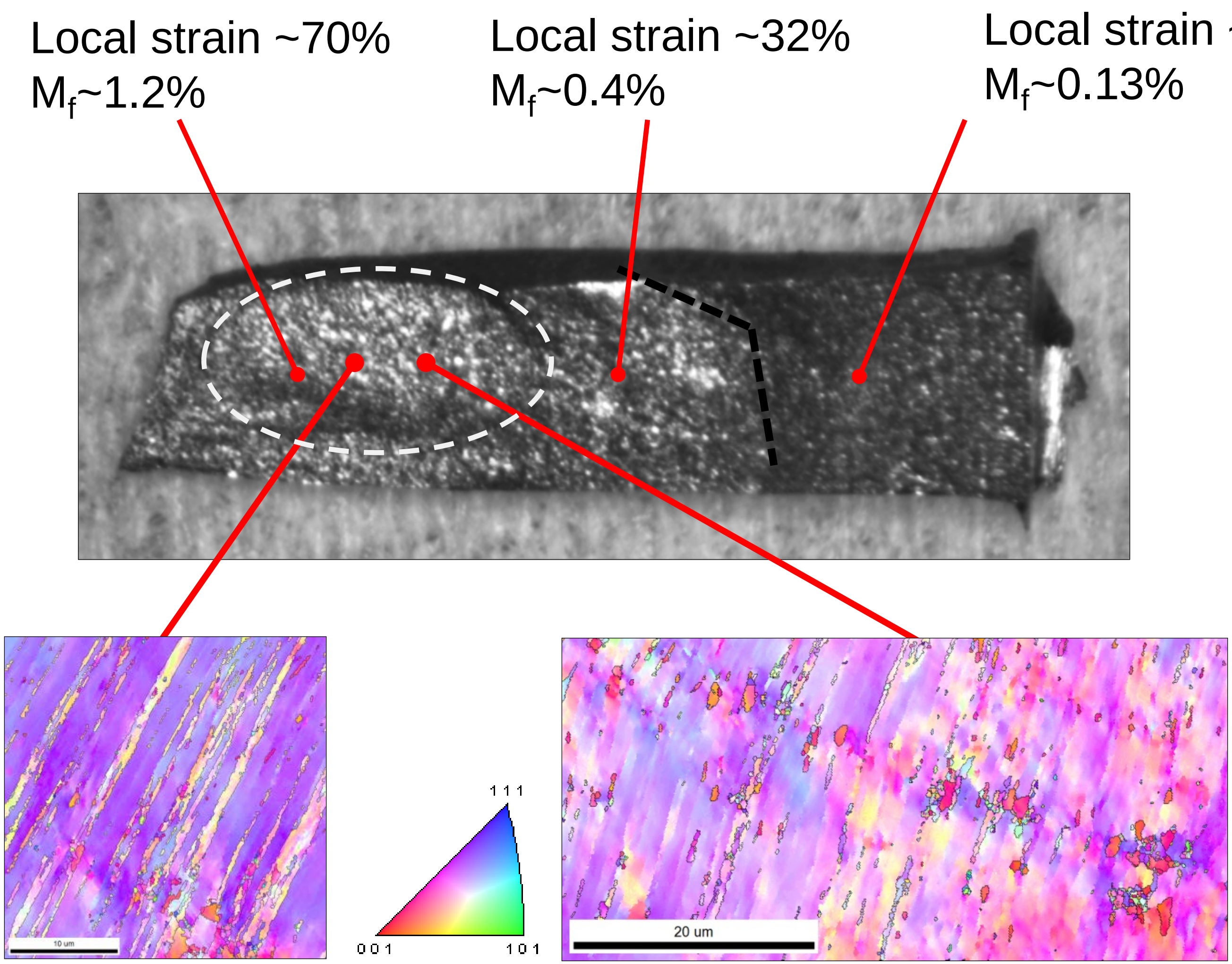

- It is possible to expect, the second scanned area consists of one large grain (shown by white oval)
- The deformed grain contains multiple deformation twins and relatively high degree of in-grain misorientation

Numerous twins and α-martensite particles were observed in deformed regions of D1-2

Local strain ~70% | Local strain ~32%

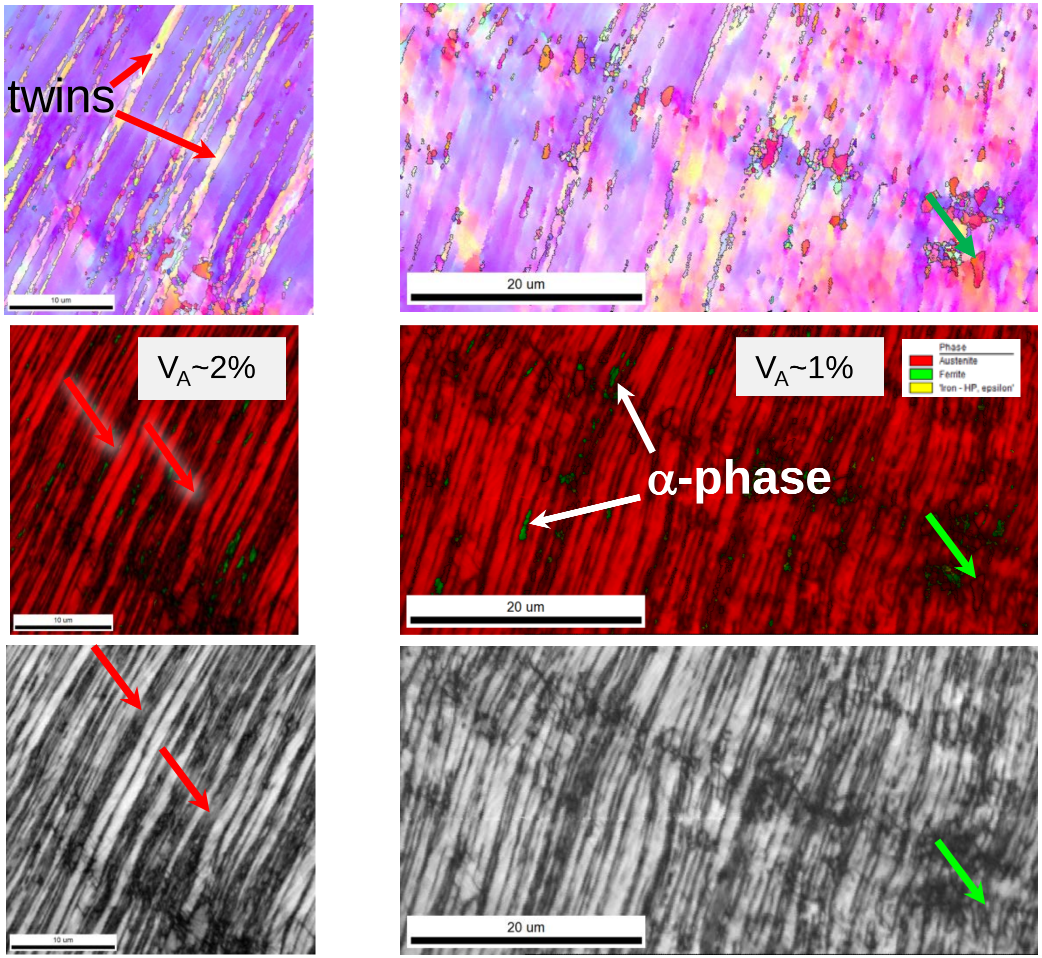

IPF, Phase+IQ, and IQ maps for large grain located close to the neck.

- The deformed grain contained multiple deformation twins (red arrows). IQ values for deformation twins are considerably lower compared to matrix.
- Also austenitic matrix contained multiple small areas with high misorientation level relative to the matrix (green arrow). Such areas formed during plastic deformation.
- Numerous alpha-martensite particles of ~2-5 micron size presented in the structure. The alpha-martensite grains were embedded in the austenitic matrix; some martensitic grains were associated with twins.
- The observation of alpha-martensite was confirmed by hand analysis of EBSD patterns. Epsilon-martensite was not observed.

The microstructure of D7-2 was more *typical* of polycrystalline 316L

Location #1
Local strain ~16%
M_f~0.4%

Location #2,
Local strain ~20%,
M_f~0.6%

Location #3,
Local strain ~66%,
M_f~2%

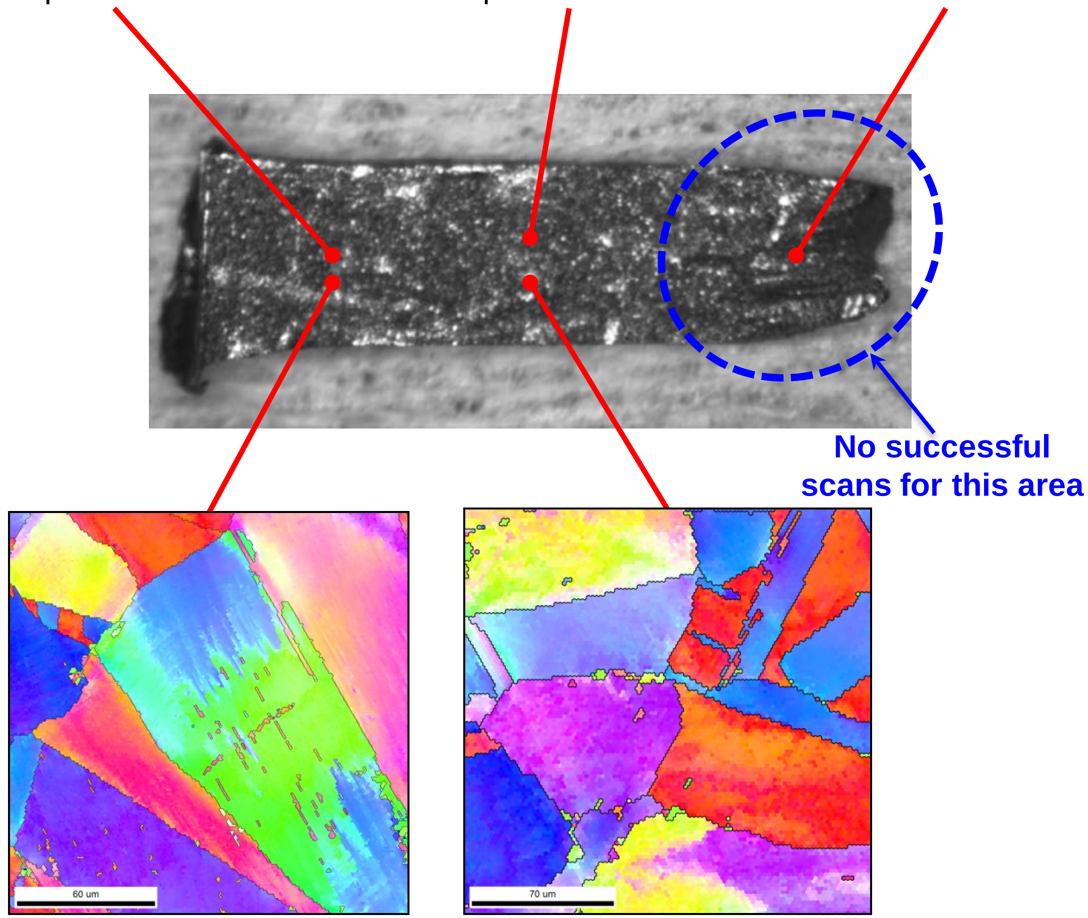

- In contrast to D1-2 specimen, in D7-2 the strain-induced relief was very weak suggesting regular (more or less) grain size.
- EBSD analysis was conducted at locations #1 and #2; no good patterns were obtained at the Location #3 (neck).
- Low-magnification scans (400x) demonstrated regular grain size at Locations #1 and #2. No coarse grains were observed in D7-2 specimen.

Deformation twins and α-martensite particles were observed in deformed regions of D7-2

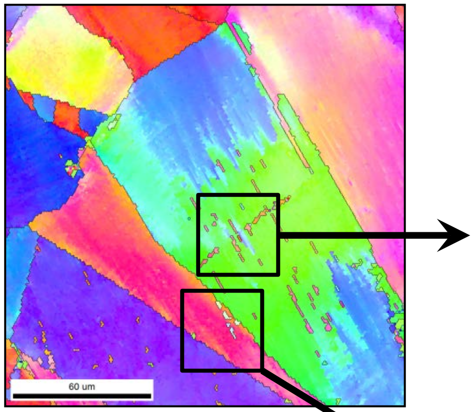

Location #1
local strain ~16%
M_f ~0.4%

- Numerous deformation twins are clear visible
- Alpha-martensite was observed as a colony (white oval) and as dispersed small particles.

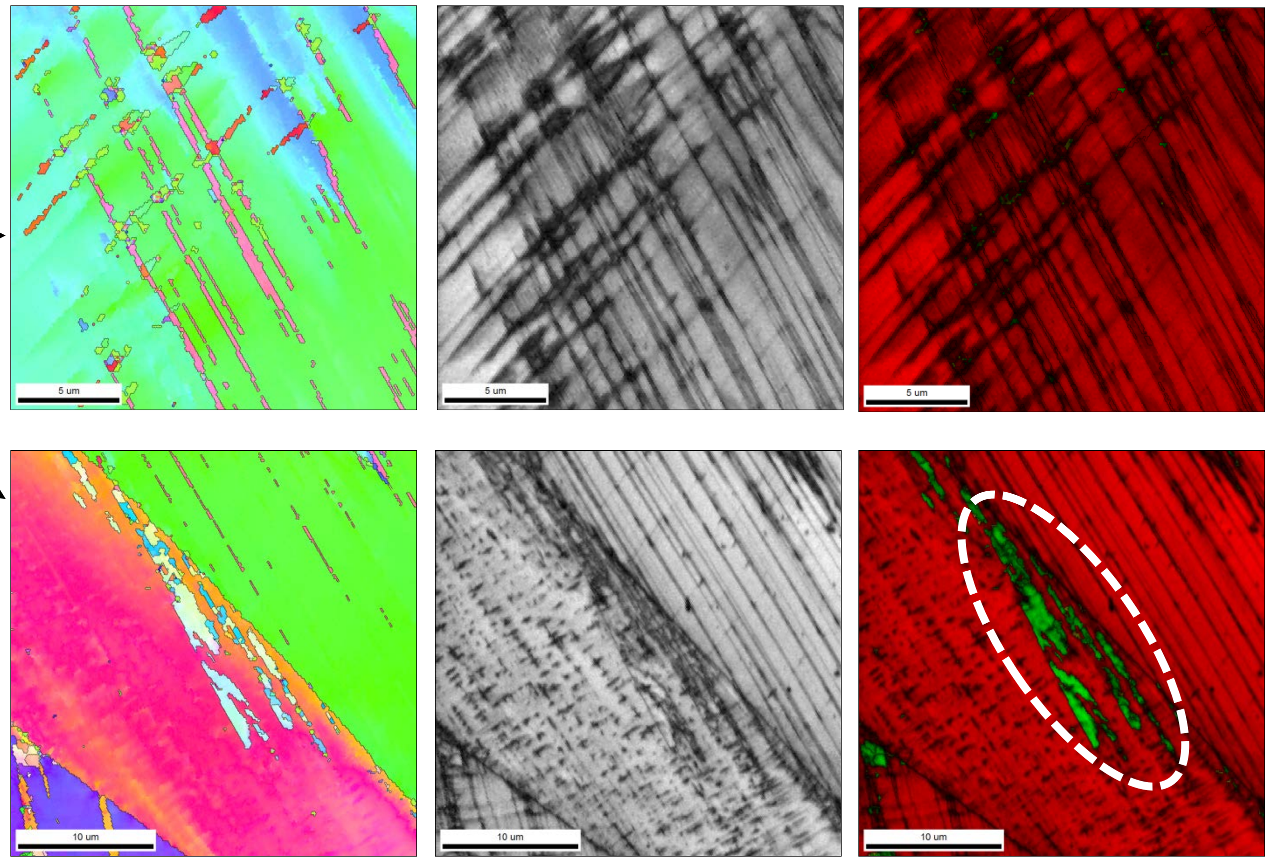

IPF, IQ, and Phase+IQ maps for two subareas of Location #1

Deformation twins and α-martensite particles were observed in deformed regions of D7-2

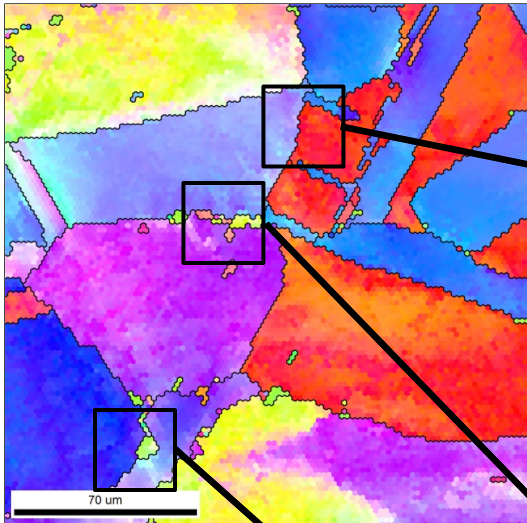

Location #2,
local strain ~20%,
M_f~0.6%.

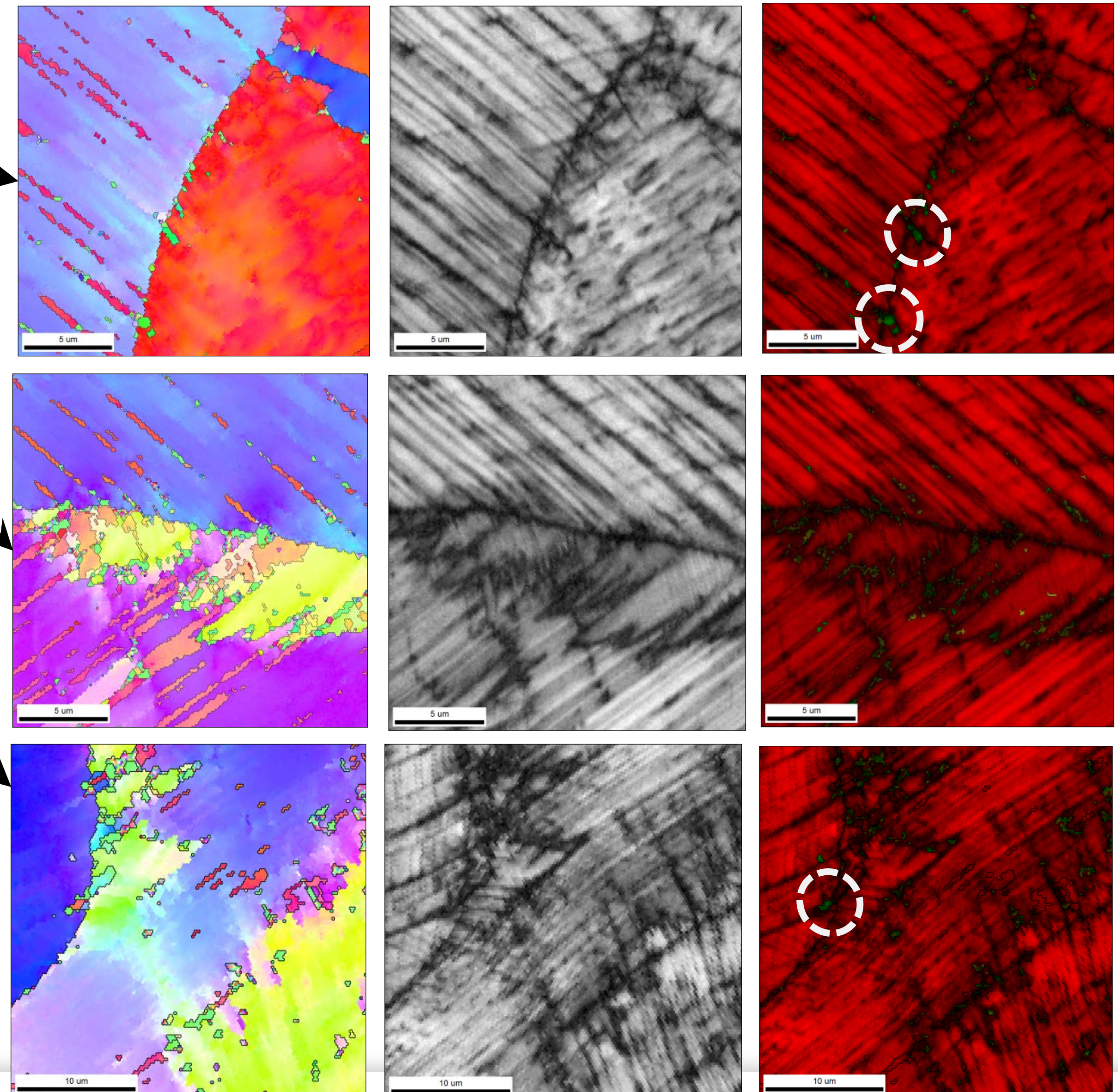

- Numerous deformation twins are clear visible
- Only small dispersed alpha-martensite particles were reliably observed

Significantly larger magnetic volume fractions were measured in D6-2

M_f~3.01,
Strain level?

M_f~1.46 (x10 times more!)
Local strain ~75-80%

M_f~0.149,
Local strain < 1%

M_f~0.148,
Local strain < 1%

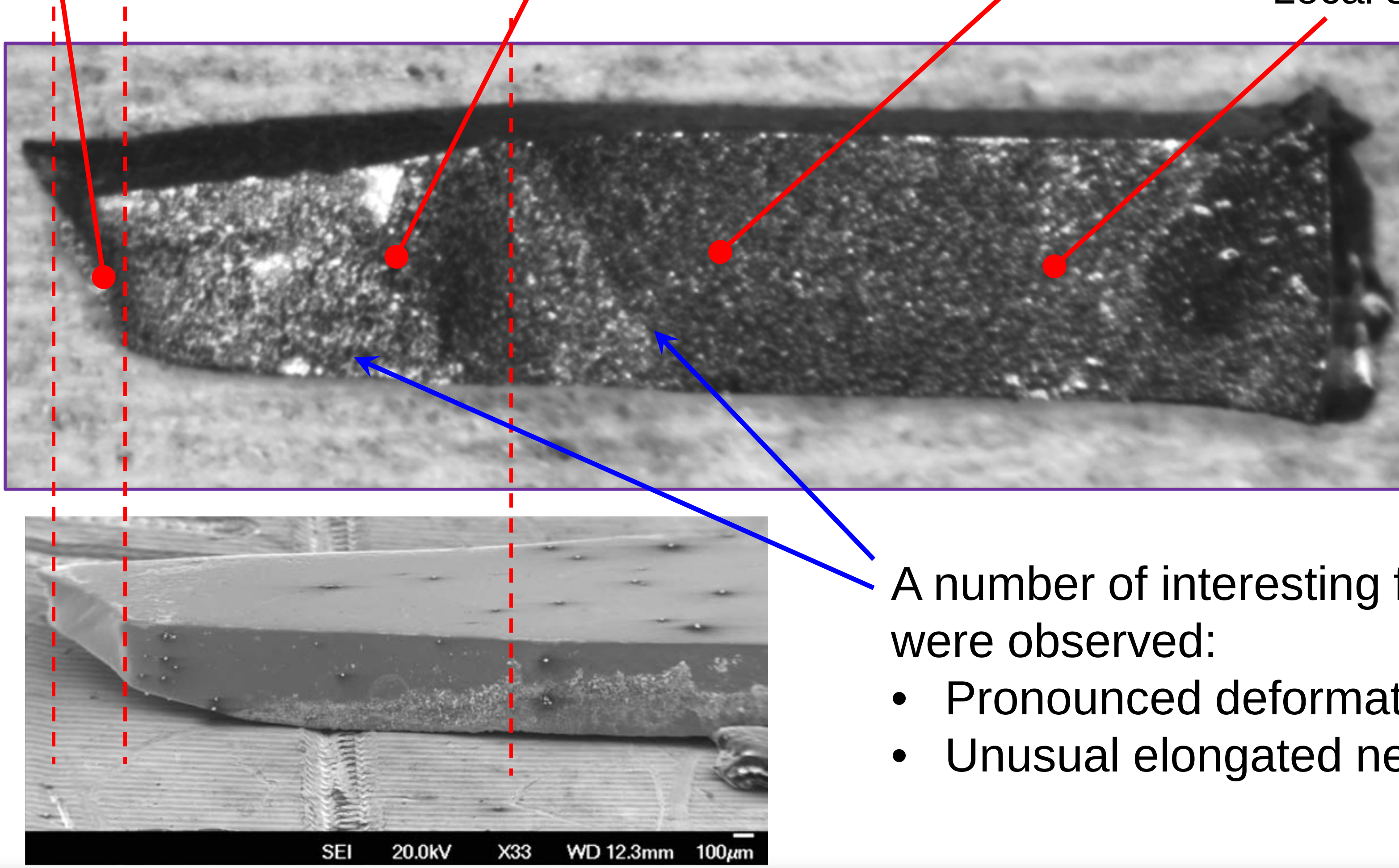

A number of interesting features were observed:

- Pronounced deformation band
- Unusual elongated neck

Evidence of a deformation wave was observed in D6-2

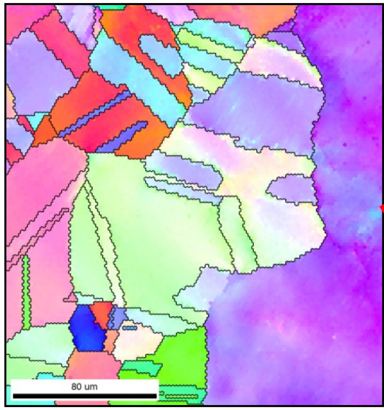

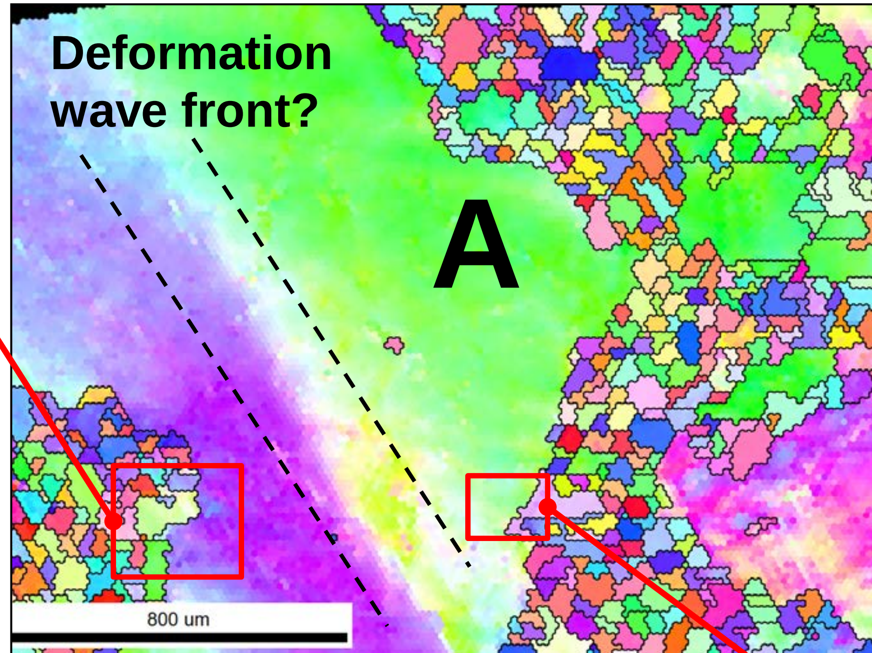

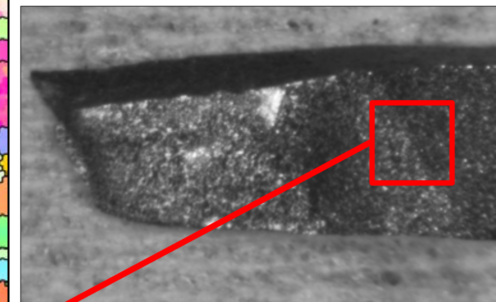

[010]

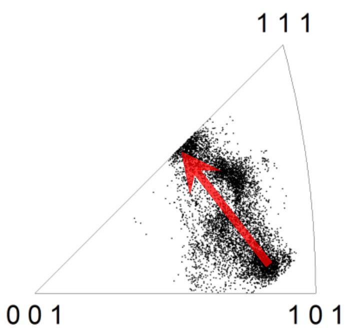

Misorientation evolution of the central grain A. It rotates towards stable [211] orientation.

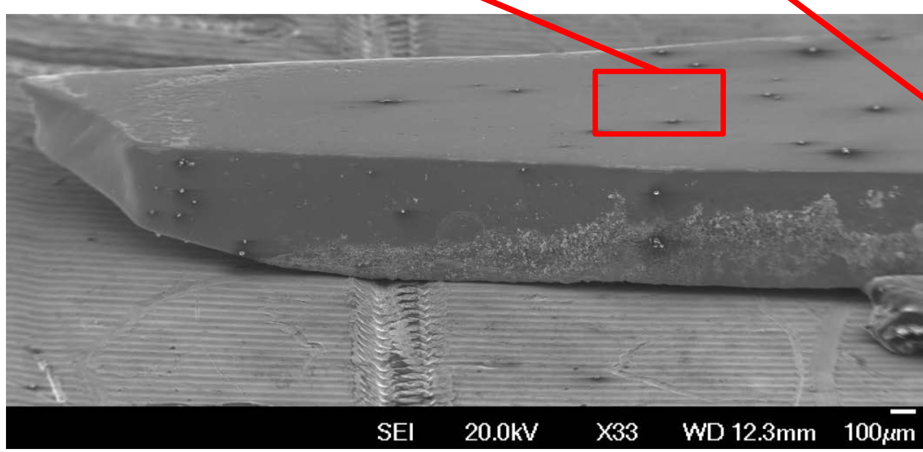

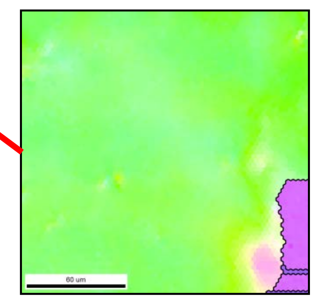

High levels of strain and misorientation were observed in D6-2

- High degree of fragmentation
- High local misorientation level
- High local strain level (~70-80%)
- Low scan rate due to low patterns quality
- High density of deformation twins

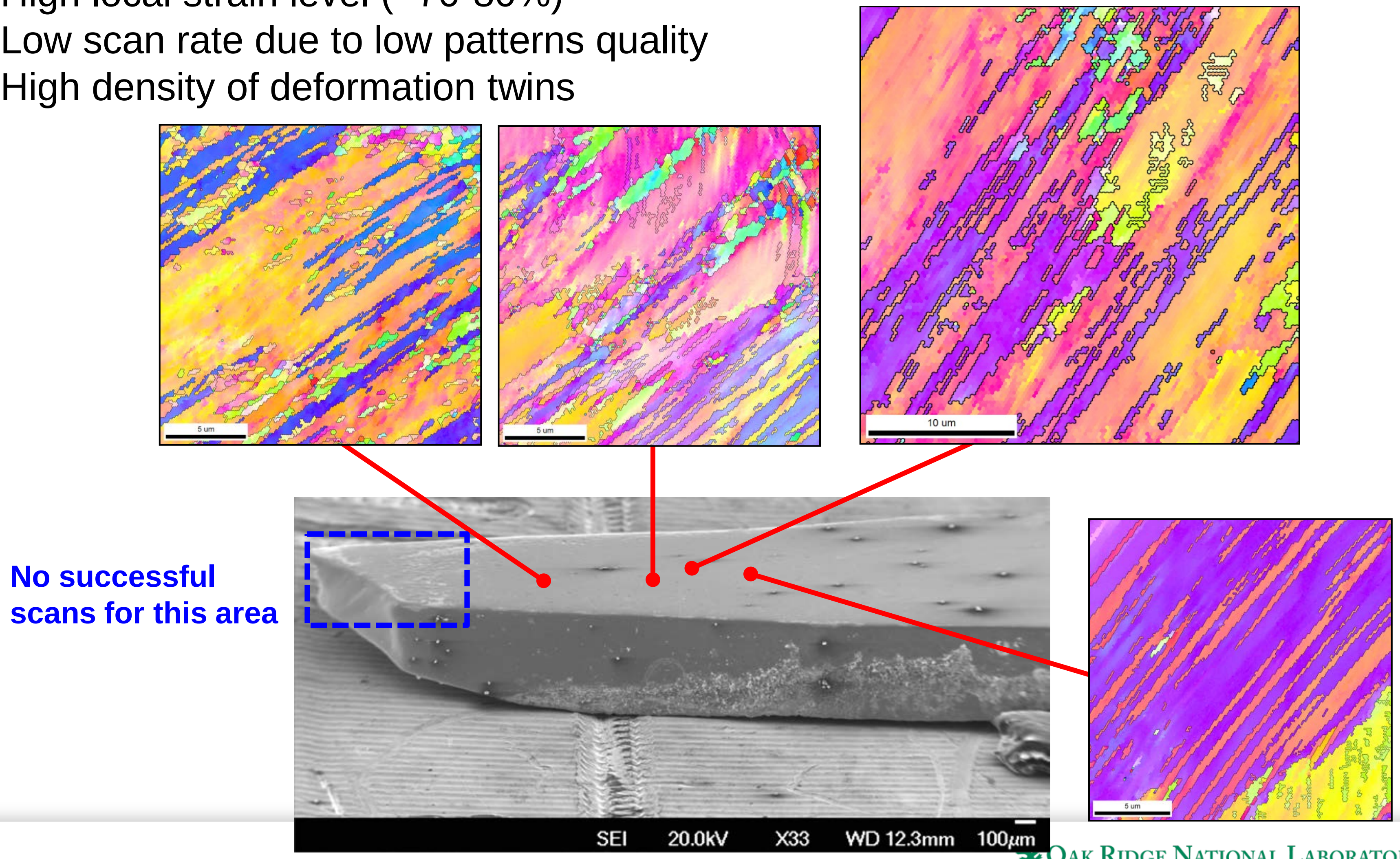

Significant volume fractions of α-martensite were observed in D6-2

- Structure contain significant amount of alpha-martensite; its amount varies along the gauge
- Neck may contain up to 25-30 % of α-martensite
- Epsilon-phase indications are non-convincing
- Martensite co-exists with twins

For all maps:
γ: Red;
α: Green;
ε: Blue.

No successful scans for this area

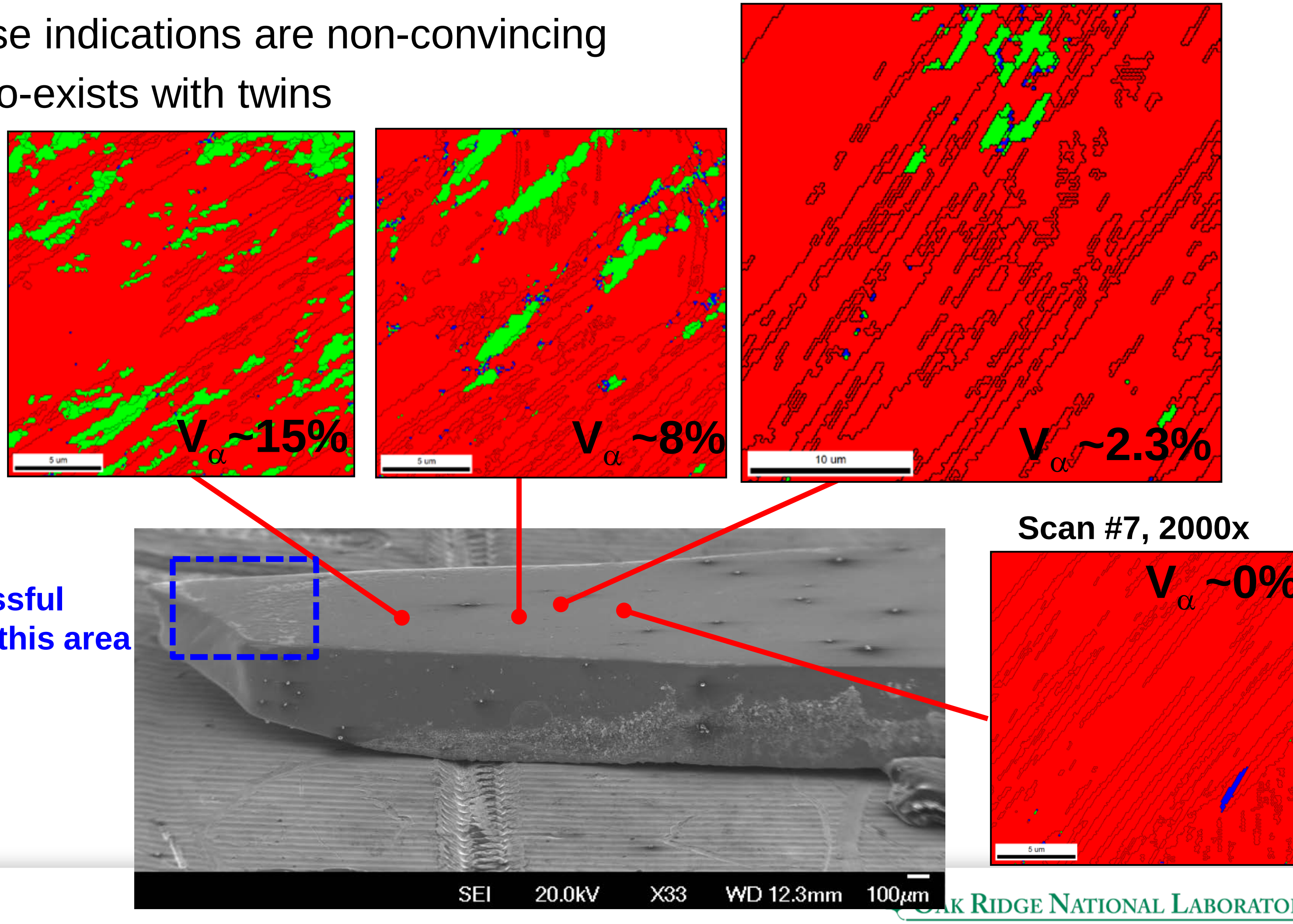

Analysis of deformation hardening

- True stress-true strain curves were created using the following relationships: $\sigma = F\times(1+\Delta L/L_0)$; $\varepsilon = \ln(1+ \Delta L/L_0)$,

  where: F = acting force, $\Delta L/L_0$ = engineering strain
- Swift equation with two free parameters was used: $\sigma = k\times(\varepsilon + \varepsilon_0)^{0.5}$ to analyze the true curves.

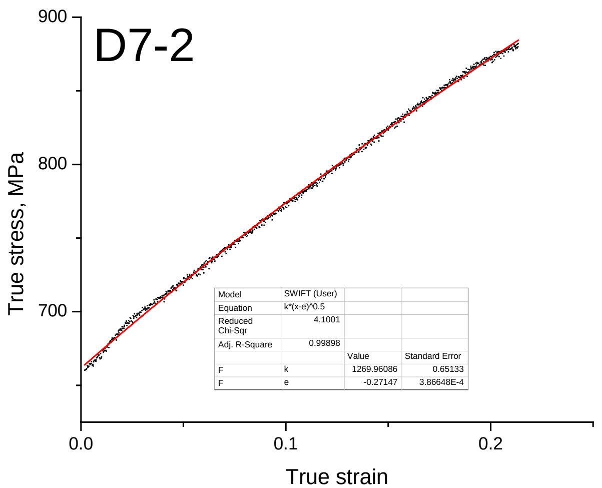

- Regular grains
- No initial force drop
- Parabolic hardening (Swift eq. works well)

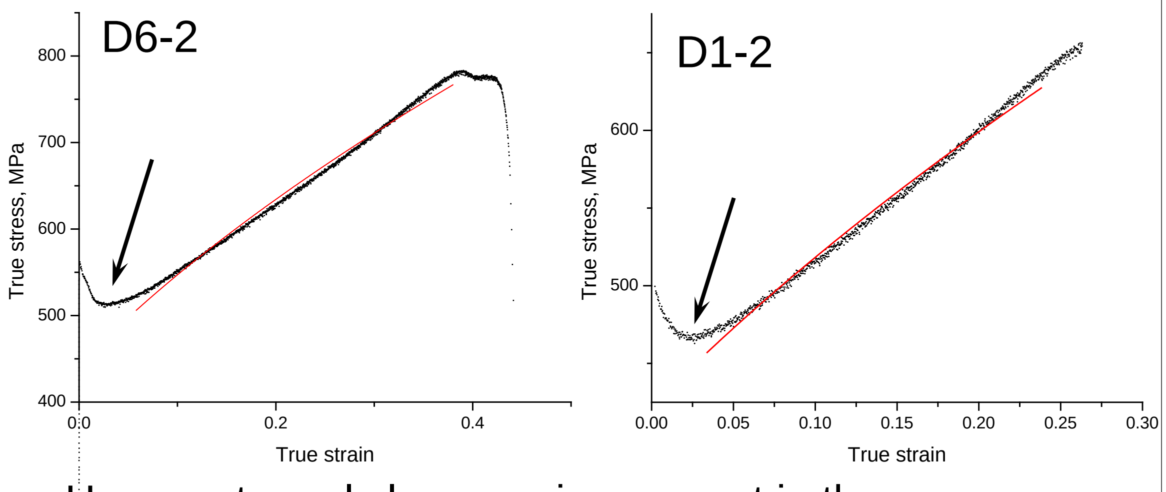

- Huge, extremely large grains present in the gauge
- Pronounced force drop
- Non-parabolic hardening (Swift eq. doesn't work)
- Deformation hardening rate increases with strain

Deformation Behavior of Specimen D6-2

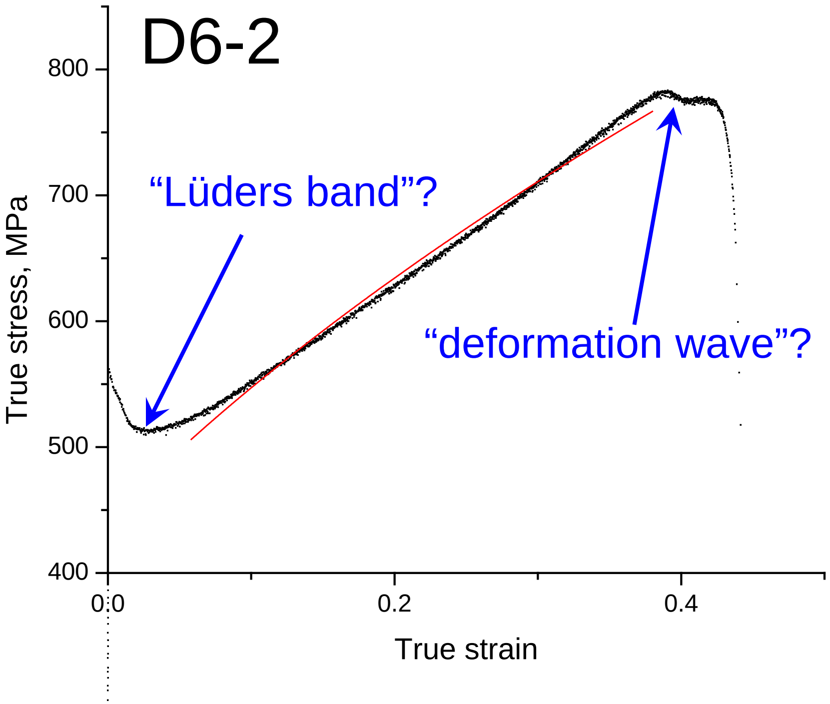

- Force drop after yield stress and structure analysis may suggest the formation of a phenomenon similar to Lüders deformation band in bcc-steels.
- Such behavior in the small strain area is caused, most probably, by large grain size.
- Also, specific necking behavior may be a sign of deformation wave caused by intensive phase transformation (known as TRIP or TWIP effects). Up to 15% of martensite was observed, more may present in the neck (one needs ~25-50% of martensite to form deformation wave.
- This phenomenon may be stimulated by a decrease in phase stability in irradiated steel compared to non-irradiated.
- Special tensile tests with optic measurements (DIC) are required to confirm this specific behavior.

D1-2 vs. D6-2: What the difference?

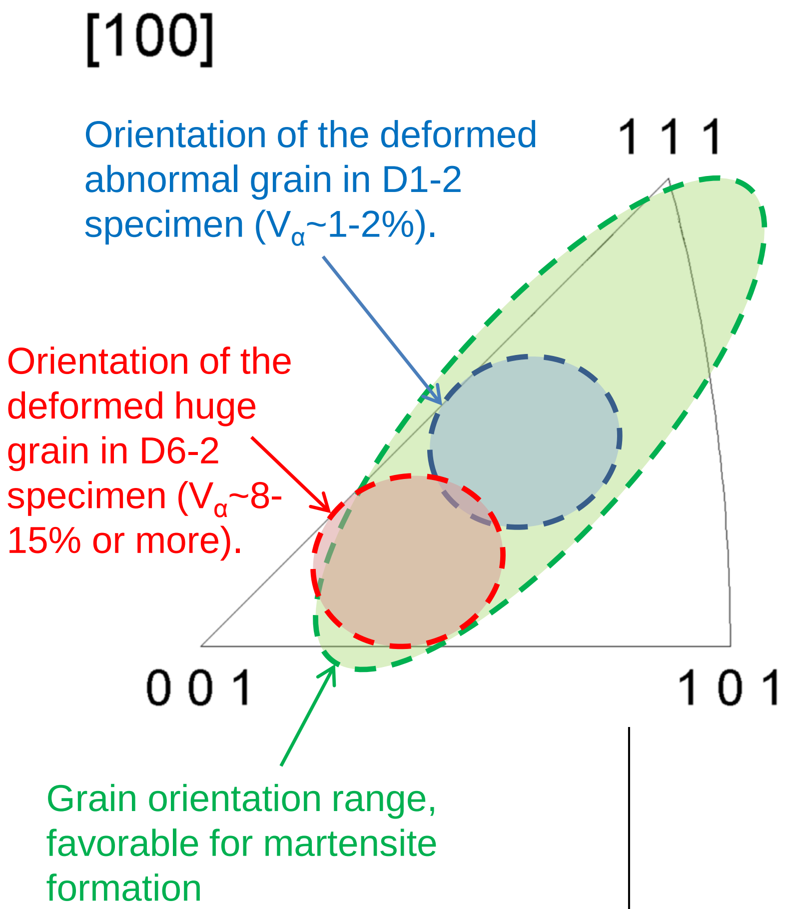

- Both twinning and martensite formation are sensitive to the orientation of grain relative to the external stress.
- For austenitic steels, deformation twinning and martensite formation is suppressed (or, at least less pronounced) in grains of [001] and ~[101] orientation.
- It appears that in the D6-2 specimen, the large grain had more favorable orientation providing more fast martensite accumulation compared to the D1-2 specimen.

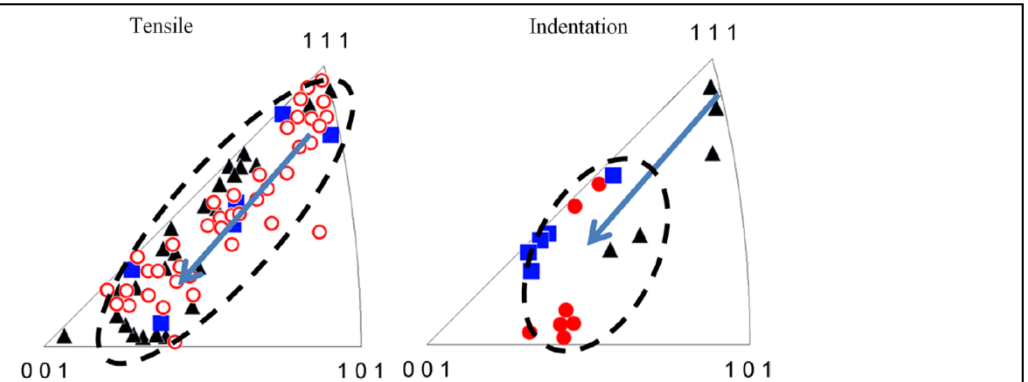

Fig. 10. Orientation of parent austenite for different types of martensite for tensile and indentation tests (triangles – separated particles; squares – line-like or chaotic shape colonies in the grain; filled circles – near-grain boundary colonies; open circles – martensite related to twins). Arrows show a tendency to increase the average amount of martensite in the grains. Dash ovals show the preferable areas of martensite formation.

Figure Reproduced From: Gussev M.N. et al., Mat. Sci. Eng. A, 2013.

Summary

- The presence of abnormal grains in the structure led to high scattering of the tensile tests results (for both strength and ductility data points).
- Large grains stimulated formation of pronounced force drop at the yield stress point.
- Twinning and phase transformation may provide additional hardening and *may* also enhance the ductility.
- Since twinning and phase transformation are strongly sensitive to grain orientation, specimens with large grains may exhibit different behavior depending on the orientation of the dominating grain(s).
- "Enhanced" ductility observed in D6-2 was likely caused by martensite formation in large grains during deformation.
- Deformation wave behavior must be verified with DIC during testing, which we intend to do in upcoming testing campaigns…coming soon.

Displacement Damage Calculations for Targets 1 and 2

134 D.A. McClintock et al./Journal of Nuclear Materials 450 (2014) 130–140

Table 1
Displacement dose calculation results for tensile specimens from SNS Targets 1 and 2.

Target	Disk	Specimen	Neutron (dpa)	Proton (dpa)	Total (dpa)	n/p
Target 1	Disk 1	D1-1	2.4	1.4	3.8	1.72
		D1-2	2.4	1.3	3.7	1.76
		D1-3	3.7	2.7	6.4	1.41
		D1-4	3.7	2.5	6.3	1.46
	Disk 6	D6-1	3.6	3.4	7.1	1.06
		D6-2	3.5	3.4	7.0	1.03
		D6-3	3.5	3.3	6.8	1.05
		D6-4	3.3	3.2	6.5	1.04
	Disk 7	D7-1	2.3	2.9	5.3	0.79
		D7-2	2.6	3.3	5.9	0.79
		D7-3	2.7	3.3	6.0	0.80
		D7-4	2.7	3.4	6.1	0.80
		D7-5	2.7	3.4	6.1	0.80
		D7-6	2.6	3.2	5.7	0.81
		D7-7	2.3	2.9	5.3	0.79
Target 2	Disk 1	D1-1	2.5	0.8	3.3	3.05
		D1-2	2.6	1.2	3.8	2.24
		D1-3	2.8	1.5	4.3	1.87
		D1-4	2.9	1.7	4.6	1.70
	Disk 6	D6-1	3.1	1.5	4.6	2.03
		D6-2	3.3	2.1	5.4	1.52
		D6-3	3.4	2.7	6.1	1.28
		D6-4	3.4	2.7	6.1	1.28
		D6-5	3.5	3.1	6.6	1.12
	Disk 7	D7-1	2.5	2.1	4.7	1.20
		D7-2	2.7	2.7	5.4	0.98
		D7-3	2.7	3.1	5.8	0.87
		D7-4	2.7	3.3	6.0	0.82
		D7-5	2.7	3.1	5.8	0.87
		D7-6	2.6	2.7	5.3	0.98
		D7-7	2.5	2.1	4.7	1.20

Displacement Damage Calculations for Targets 1 and 2

Table 2
Simulation results for H and He concentration in tensile specimens from SNS Targets 1 and 2.

			Hydrogen production (appm)			Helium production (appm)		
Target	Disk	Specimen	Neutron [H]	Proton [H]	Total [H]	Neutron [He]	Proton [He]	Total [He]
Target 1	Disk 1	D1-1	161	940	1101	23	222	245
		D1-2	159	907	1066	23	214	237
		D1-3	275	1797	2073	40	424	465
		D1-4	274	1723	1997	40	407	447
	Disk 6	D6-1	253	2363	2616	37	566	603
		D6-2	242	2366	2607	36	567	603
		D6-3	238	2274	2512	35	545	580
		D6-4	230	2190	2420	34	525	559
	Disk 7	D7-1	151	2039	2191	22	493	515
		D7-2	168	2266	2433	25	548	573
		D7-3	178	2317	2495	26	560	586
		D7-4	177	2367	2544	26	572	598
		D7-5	173	2349	2521	25	568	594
		D7-6	167	2200	2366	25	532	557
		D7-7	151	2042	2193	22	493	515
Target 2	Disk 1	D1-1	161	560	720	23	134	157
		D1-2	177	811	988	26	195	221
		D1-3	198	1047	1245	29	252	281
		D1-4	207	1191	1398	30	288	318
	Disk 6	D6-1	201	1063	1265	29	258	288
		D6-2	218	1509	1727	32	369	401
		D6-3	237	1901	2139	35	466	501
		D6-4	240	2213	2453	35	543	578
		D6-5	248	2344	2592	36	575	611
	Disk 7	D7-1	161	1510	1671	23	373	396
		D7-2	173	1939	2112	25	480	505
		D7-3	181	2216	2397	26	549	575
		D7-4	173	2346	2519	26	581	606
		D7-5	175	2211	2386	26	548	573
		D7-6	168	1907	2075	25	472	496
		D7-7	159	1504	1662	23	372	395

Mercury enters through side supply passages and returns through the center return passage

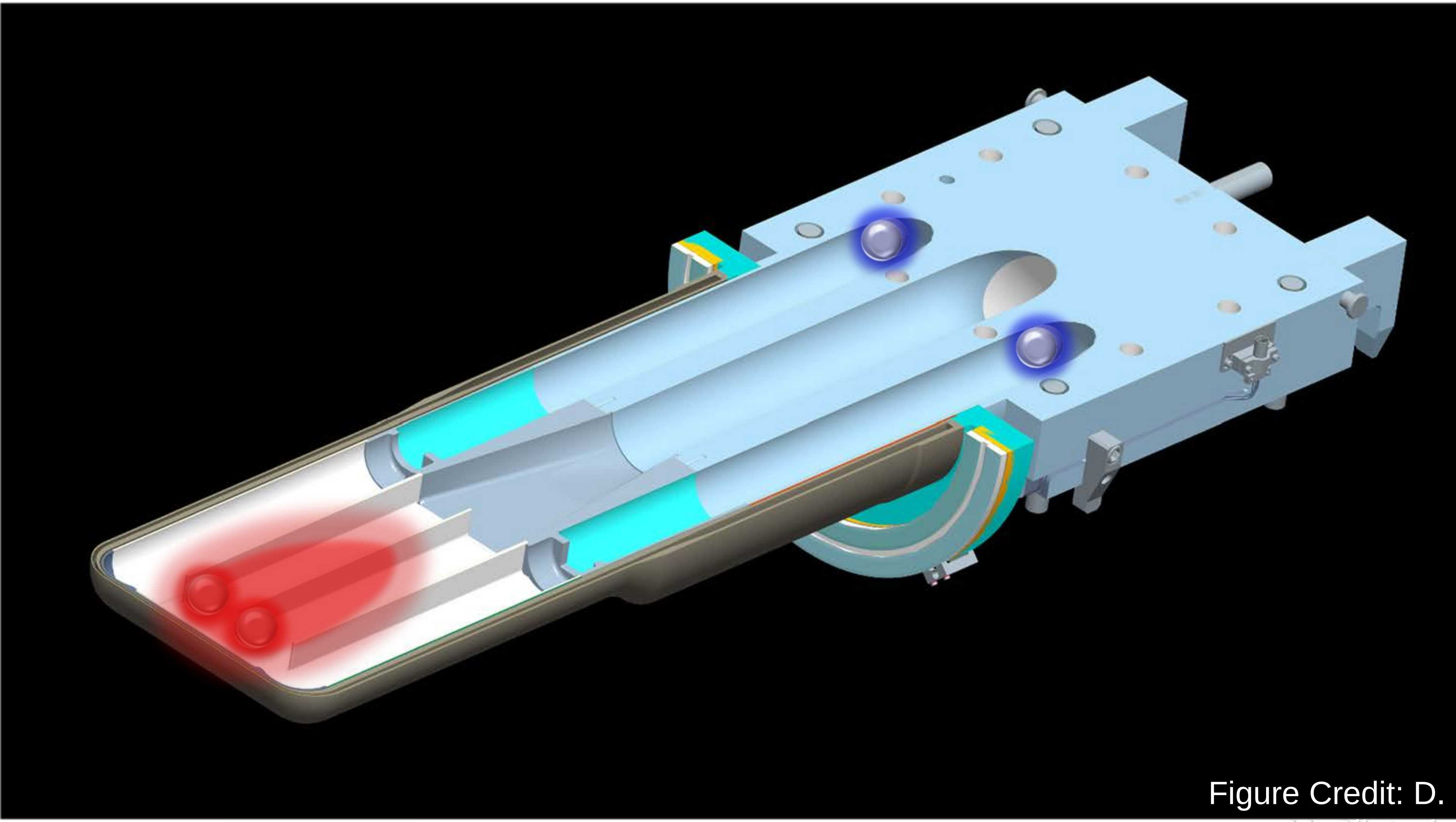

Figure Credit: D. McClintock

16 instruments are currently installed at the SNS

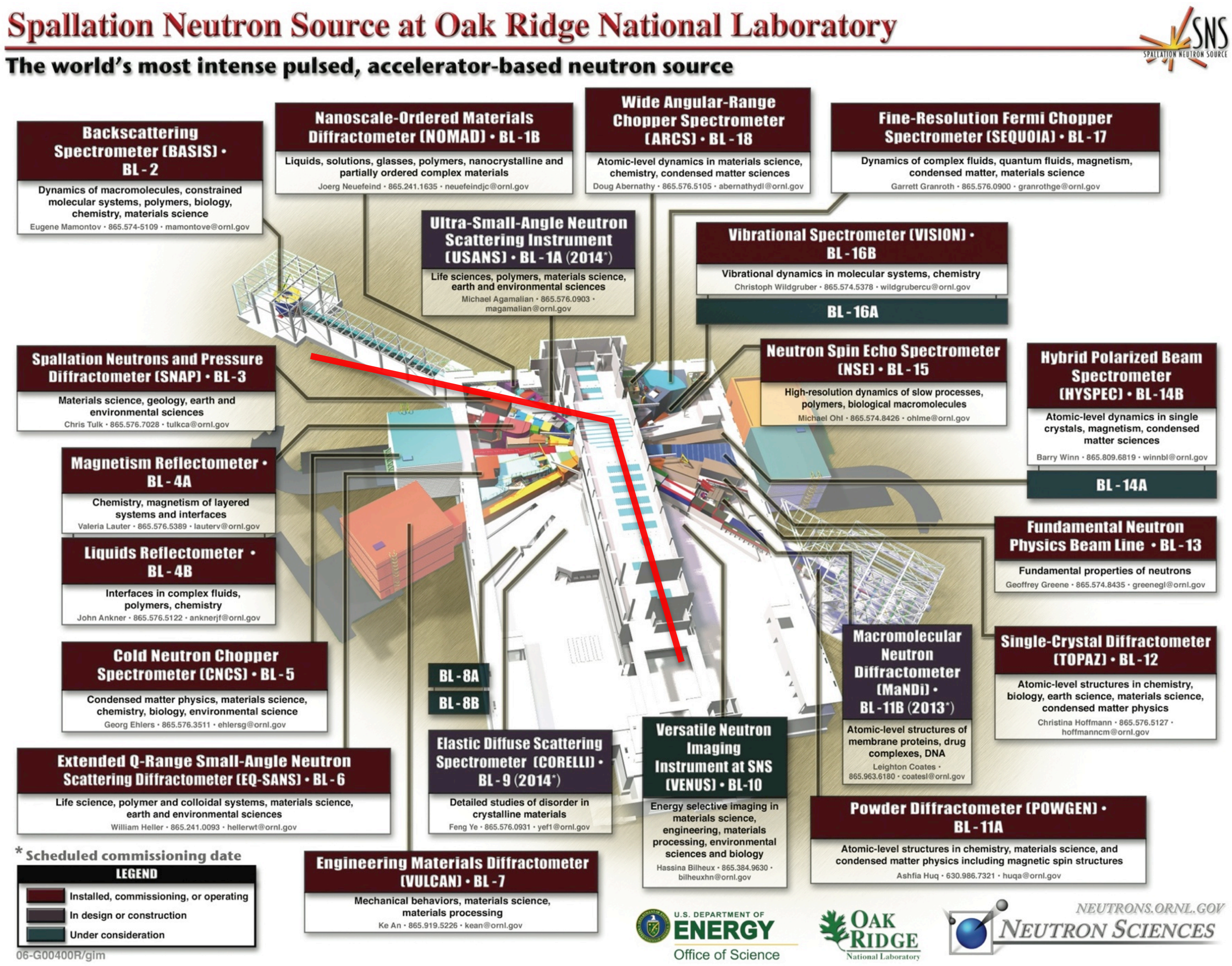

The target is inserted into a large monolith structure during operation

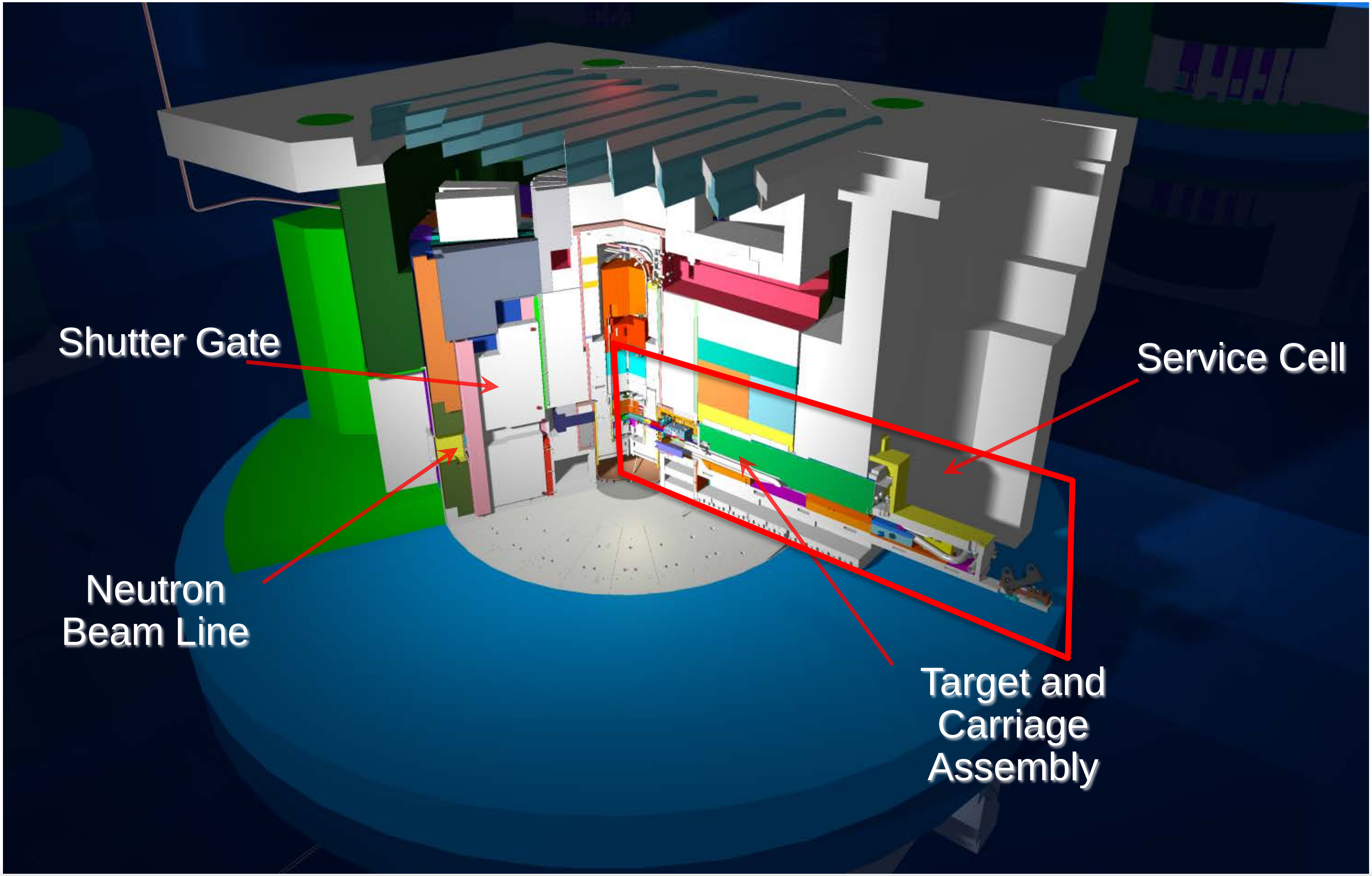

The SNS target is inserted into the operating position by a target transport carriage

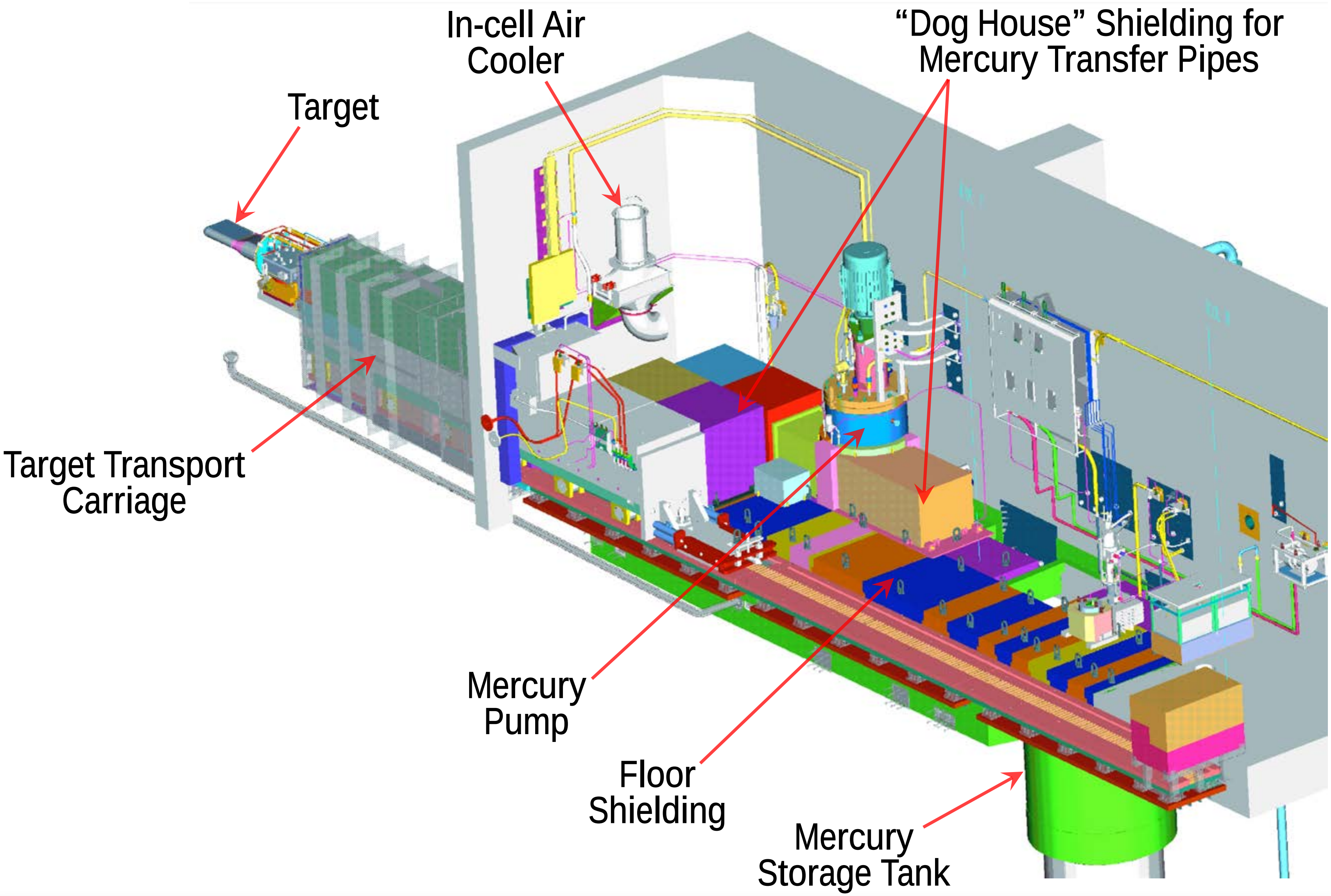

Mercury process loop circulates a mercury inventory of approximately 23 tons during operation

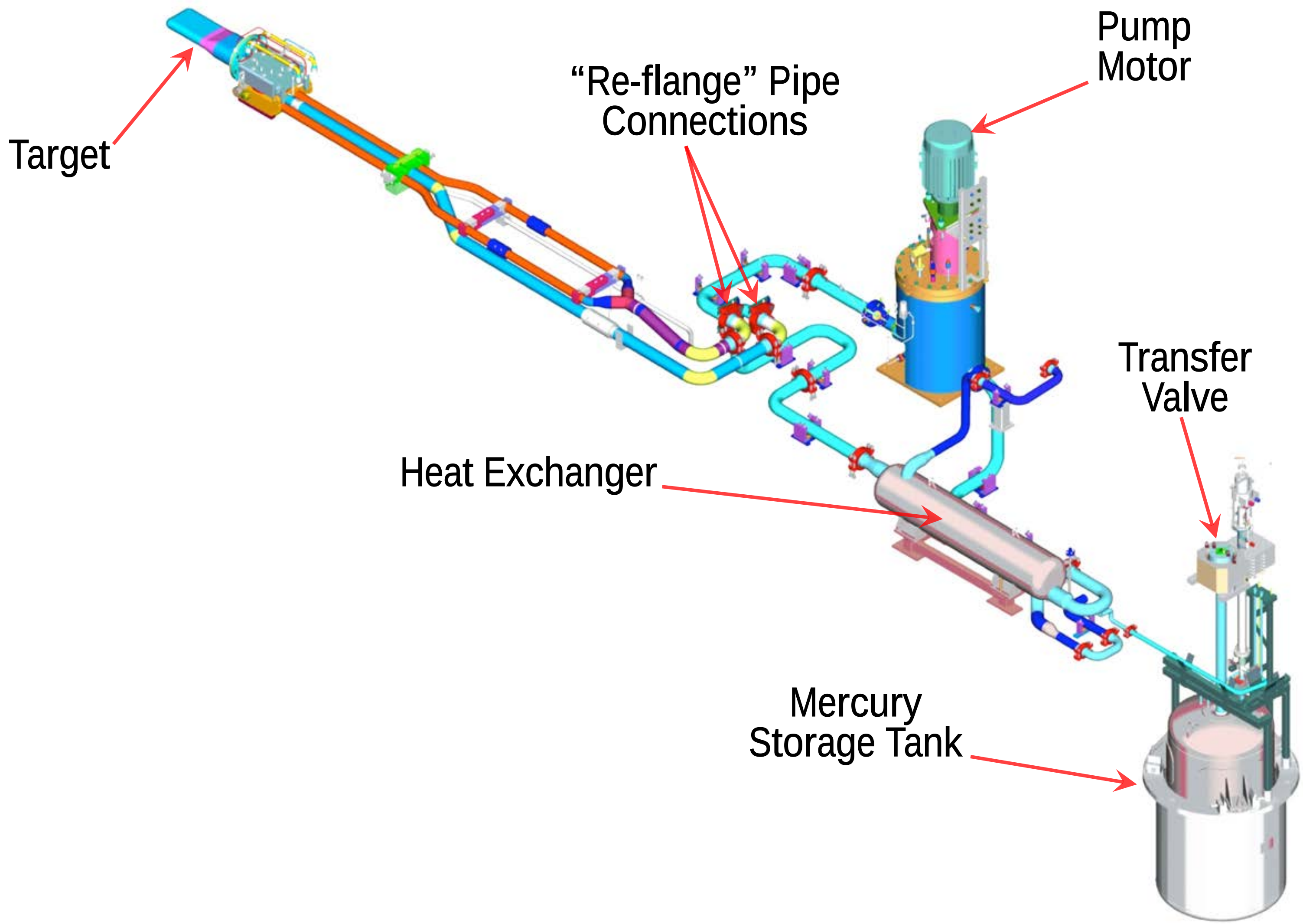

SNS target is composed of two "vessels" welded to a manifold block

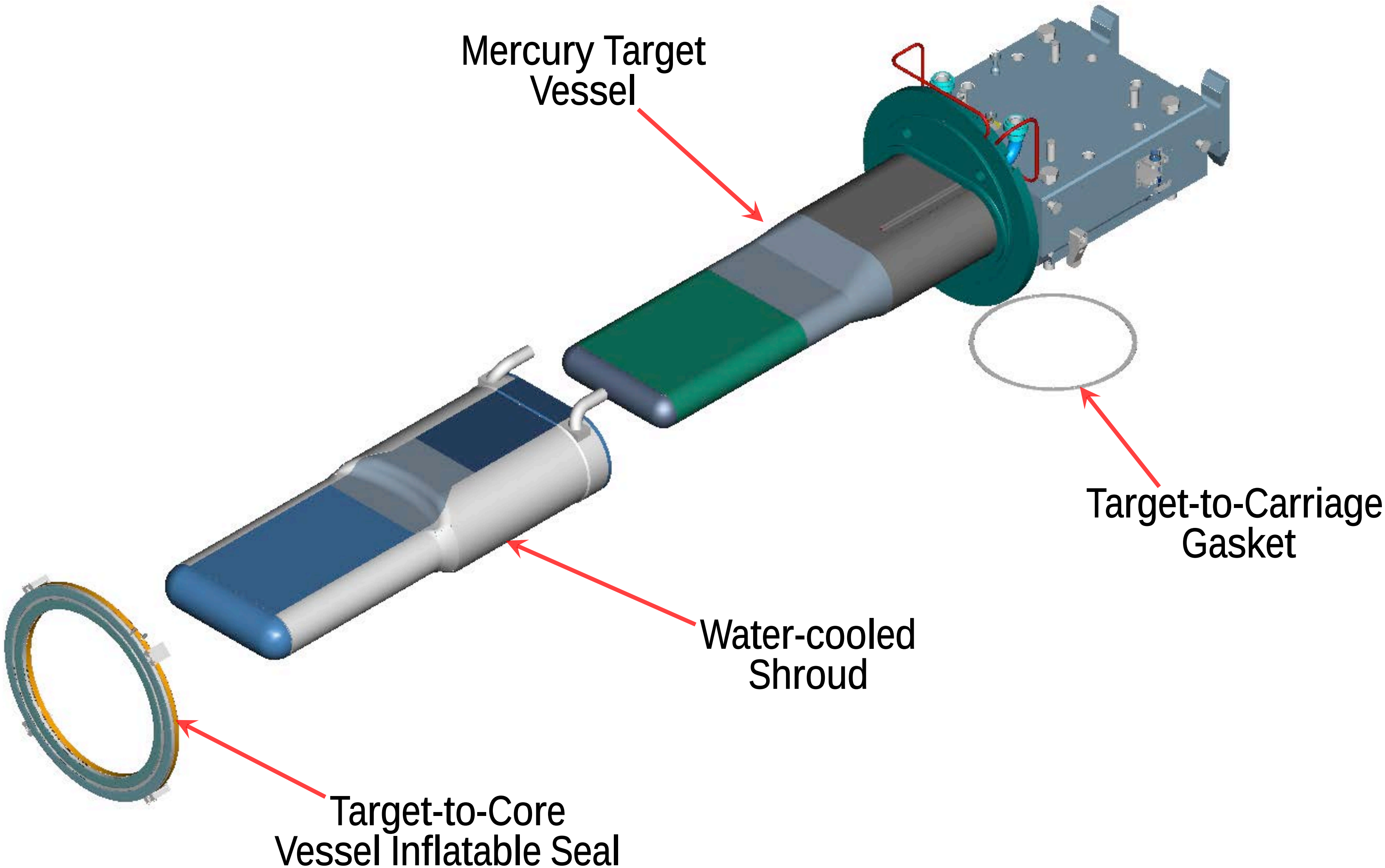

The SNS Target module transports mercury to and from the neutron generation zone

- The SNS Target is a liquid metal design – utilizing flowing mercury (23 L/sec) as the neutron producing “target” material
- Target vessel and water-cooled shroud are composed of AISI 316L austenitic stainless steel